OAK RIDGE NATIONAL LABORATORY LIBRARIES
3 4456 0555907 1
OAK RIDGE NATIONAL LABORATORY LIBRARIES

CENTRAL RESEARCH LIBRARY

ORNL-TM-4585

Cy 2

ENERGY CONTAINMENT AND SCALING IN TOKAMAKS

(The Phylogony of a Tokamak Discharge)

J. F. Clarke

OAK RIDGE NATIONAL LABORATORY
CENTRAL RESEARCH LIBRARY
DOCUMENT COLLECTION
LIBRARY LOAN COPY
DO NOT TRANSFER TO ANOTHER PERSON
If you wish someone else to see this document, send in name with document and the library will arrange a loan.
UCN-7969
(3 3-67)

OAK RIDGE NATIONAL LABORATORY
OPERATED BY UNION CARBIDE CORPORATION • FOR THE U.S. ATOMIC ENERGY COMMISSION

This report was prepared as an account of work sponsored by the United States Government. Neither the United States nor the United States Atomic Energy Commission, nor any of their employees, nor any of their contractors, subcontractors, or their employees, makes any warranty, express or implied, or assumes any legal liability or responsibility for the accuracy, completeness or usefulness of any information, apparatus, product or process disclosed, or represents that its use would not infringe privately owned rights.

ORNL-TM-4585

Contract No. W-7405-eng-26

THERMONUCLEAR DIVISION

ENERGY CONTAINMENT AND SCALING IN TOKAMAKS
[The Phylogony of a Tokamak Discharge]

J. F. Clarke

L. A. Artsimovich Memorial Lecture
Presented at the American Physical Society Meeting
Division of Plasma Physics
Philadelphia, Pennsylvania
October 30-November 3, 1973

MAY 1974

NOTICE This document contains information of a preliminary nature and was prepared primarily for internal use at the Oak Ridge National Laboratory. It is subject to revision or correction and therefore does not represent a final report.

OAK RIDGE NATIONAL LABORATORY
Oak Ridge, Tennessee 37830
operated by
UNION CARBIDE CORPORATION
for the
U.S. ATOMIC ENERGY COMMISSION

OAK RIDGE NATIONAL LABORATORY LIBRARIES

3 4456 0555907 1

Artsimovich Memorial Lecture

Presented at the APS-DPP Meeting, Philadelphia, 10/30-11/3-73

ENERGY CONTAINMENT AND SCALING IN TOKAMAKS
[The Phylogony of a Tokamak Discharge]

J. F. Clarke
Oak Ridge National Laboratory
Oak Ridge, Tennessee

The topic of energy containment and scaling in Tokamaks is an appropriate one for the Artsimovich Memorial Lecture because it was Academician Artsimovich who provided two fundamental insights in this area which have enabled us to draw conclusions from the experimental results. In this Lecture we shall first examine the electron energy balance as it is observed in Tokamak experiments and will show that the qualitative dependence of electron energy containment on plasma parameters is a result of microscopic energy transfer by a diffusion process which can be characterized by the pseudoclassical diffusion coefficient. This coefficient has the form of an effective collision frequency multiplied by the poloidal gyroradius squared. We will then address the question of ion energy balance as observed in the experiments and conclude that the ion energy containment in Tokamaks is the result of a balance between electron heating and the loss processes of charge exchange, particle diffusion and neo-classical ion thermal conductivity.

Measurements of time dependent electron and ion density and temperature profiles in individual discharges with precisely defined initial condition provide the most informative data for evaluating our theoretical models of Tokamak plasma behavior. Such studies form the basis of the ontogeny of a Tokamak discharge.[1] Unfortunately, these studies are as

yet incomplete and we will adopt an alternative approach in this lecture. We will examine the variation of the poloidal beta, the energy containment time, and the peak ion temperature, which are parameters describing the gross behavior of Tokamak discharges, as observed on several different Tokamak experiments over a wide range of initial conditions. The parametric variation of these quantities provides an indication of the nature of the major energy transfer processes in Tokamak devices. This study constitutes a phylogony of Tokamaks.

I. SCALING WITH PSEUDOCLASSICAL THERMAL CONDUCTIVITY

First, let us turn to the question of the electron energy balance. When Academician Artsimovich considered this problem he assumed that the energy input to the electrons from ohmic heating was balanced by an energy loss by means of electron thermal conductivity.[2] This balance is

$$\left(\frac{m\nu}{e^2 n}\right) J^2 = \frac{1}{r}\frac{\partial}{\partial r} r n_e \kappa_e \frac{\partial T_e}{\partial r} \tag{1}$$

where we have written the plasma resistivity in terms of its constituent parts in order to emphasize its dependence on the electron collision frequency ν. In order to arrive at the parametric dependence of the electron thermal conductivity κ_e Academician Artsimovich replaced the derivatives on the right hand side of Equation 1 by a scale length which we denote here by a constant c_0 multiplied by the radius of the plasma a. This yields

$$\left(\frac{m\nu}{e^2 n}\right) J^2 = \frac{n_e T_e \kappa_e}{(C_0 a)^2} \tag{2}$$

In solving for the electron thermal conductivity we arrive at Equation 3

$$\kappa_e = \frac{16\ C_0^{\ 2}}{\beta_p^{\ 2}}\ \nu\rho_p^{\ 2} \tag{3}$$

where we have defined the β_p as the energy content of the plasma divided by the square of the magnetic field due to the plasma current. The fundamental insight of Academician Artsimovich consisted in noting that the experimentally measured values of beta poloidal were approximately constant and equal to 1/2.[3] If we take beta poloidal in Equation 3 equal to a constant we arrive at an electron thermal conductivity coefficient which has the pseudoclassical form of collision frequency times the poloidal gyroradius squared. The constant in the expression for the electron thermal conductivity was determined by using the experimentally determined electron temperature gradient in Equation 1 along with an electron thermal conductivity coefficient of the pseudoclassical form. This procedure gave a coefficient of 10.

$$\kappa_e = 10\ \nu\rho_p^{\ 2} \tag{4}$$

At roughly the same time that Academician Artsimovich proposed the pseudoclassical form for the electron thermal conductivity, Yoshikawa[4] proposed a particle diffusion coefficient with the same pseudoclassical form.

$$D_{pc} \propto \nu\rho_p^{\ 2} \tag{5}$$

This particle diffusion coefficient was based on a theoretical analysis of the effect of drift modes on particle transport rather than on an analysis of the experimental observations and the coefficient was left undetermined.

If we accept for the moment that the electron energy loss from the plasma is determined by a thermal diffusion process with a diffusion coefficient of the pseudoclassical form how will the experimentally observable parameters vary? There are two experimentally observable parameters whose behavior is most obvious. First, the poloidal beta must be a constant. Secondly, the gross energy containment time should be given by the scale length $(c_0 a)^2$ divided by the pseudoclassical diffusion coefficient. From this we conclude that the gross energy containment time should scale like $T_e^{1/2} I^2$. In fact, neither of these consequences of pseudoclassical diffusion is observed in the experiment. At the time of his original analysis, Academician Artsimovich noted that there were deviations from constant beta poloidal in the experiment and over the years the most commonly quoted scaling law obtained from the Russian experiments is given as energy containment time proportional to the plasma current.[5] Thus, on the surface there appears to be a contradiction between the results of experiments and the predictions of pseudoclassical scaling. On the other hand, simulation of plasma behavior through use of computer codes using these pseudoclassical diffusion coefficients has been quite successful in describing the results of individual experiments.[6,7] This is illustrated in Figures 1 and 2. In these computer simulations the coefficient of the electron thermal conductivity is taken to be 3, whereas the coefficient of the electron particle diffusion is

taken to be 10. Therefore, for similar temperature and density gradients, the best fit to the experimental data is obtained by assuming that particle diffusion and not electron thermal conductivity is the dominant energy loss process from the electrons. In the rest of this section we will show that the dominance of pseudoclassical particle diffusion over pseudoclassical thermal conductivity will lead naturally to the conclusion that beta poloidal is a variable and that the electron energy containment time should scale with the current as observed in the experiments and the computer simulations.

Figure 3 shows a compilation of data taken from four Tokamak experiments, two in the Soviet Union and two in the United States.[8,9,10,11] The vertical axis represents the plasma energy content per unit length. The horizontal axis is the plasma current. On such a plot, beta poloidal equal to a constant is represented by a straight line. As is obvious from the data, there is a significant departure of beta poloidal from the constant value of a half. In fact, this departure from a constant value of beta poloidal is not random and Figure 4 shows the parametric dependence of the variation of beta poloidal. These data were taken on the ORMAK experiment[12] and they show that beta poloidal is a linear function of density and is inversely related to the current flowing in the plasma. Similar data have been obtained on the T-4[9] and ST[13] experiments.

II. SCALING WITH PSEUDOCLASSICAL PARTICLE DIFFUSION

To see how such a dependence can result from pseudoclassical diffusion we will assume that the pseudoclassical particle diffusion dominates

the energy loss of the electrons in the plasma. The electron energy balance is then represented by

$$\frac{1}{r}\frac{\partial}{\partial r} rT_e D_{pc} \frac{\partial n_e}{\partial r} = \eta J^2 \tag{6}$$

However, unlike the situation described by Equation 1, in which electron thermal conductivity dominates the electron energy balance, we must now simultaneously satisfy particle balance. Here the particle balance is maintained by the ionization of neutral particles in the plasma.

$$\frac{1}{r}\frac{\partial}{\partial r} rD_{pc} \frac{\partial}{\partial r} n_e = n_0 n_e \quad \langle\sigma_i v_e\rangle \tag{7}$$

Equations (6) and (7) can be simultaneously satisfied if we use Equation 7 to define a density gradient scale length r_n. Replacing the derivatives in Equation 7 by the scale length r_n we obtain

$$\frac{D_{pc} n_e}{r_n^{\,2}} = n_0 n_e \quad \langle\sigma_i v_e\rangle \tag{8}$$

which can be solved for the r_n:

$$r_n = \sqrt{\frac{D_{pc}}{n_0 \langle\sigma_i v_e\rangle}} \tag{9}$$

Notice that now, rather than being a constant, the scale length for the diffusion process is itself a function of the diffusion coefficient and also of the neutral density within the plasma.

The variation of the density scale length to be expected in the experiments is illustrated in Figure 5 which shows the variation in the

plasma density profile as current is varied for a fixed particle source. Referring to Equation 9 we can see that as the particle diffusion coefficient is reduced by increasing the plasma current, the scale length of the density gradient decreases, thereby leading to an increase in the diffusive energy loss described by Equation 6. From Equation 6 it is obvious that a change in the density gradient is just as important in the energy balance as a change in the diffusion coefficient.

Let us define the pseudoclassical diffusion coefficient in the form given by

$$D_{pc} = C\alpha\nu_{ei}\rho_p^{\,2} \tag{10}$$

where alpha is the resistivity anomaly factor and ν_{ei} is the electron ion collision frequency and C is a constant. Then using this definition of the pseudoclassical diffusion coefficient in Equation 6 and replacing the derivatives with our density scale length defined by Equation 9, we can solve for the energy content of the plasma n_eT_e. The result is

$$n_eT_e = \frac{r_n JB_p}{\sqrt{2\ C}} \tag{11}$$

Since we are interested in the poloidal beta variation, which is measured experimentally, we must average this plasma energy content over the volume of the plasma. Replacing r_n in Equation 11 by its definition from Equation 9 and averaging over the volume of the plasma, we arrive at

$$\langle n_eT_e\rangle = \frac{10^4}{\sqrt{\langle\sigma_i v_e\rangle}} \int_0^1 \frac{x\,dx}{T_e^{\,1/4}}\, J \sqrt{\frac{\alpha n_e}{n_0}} \tag{12}$$

The mean ionization rate $\langle\sigma_i v_e\rangle$ is approximately a constant for a wide range of electron temperatures. The remaining parameters T_e, the current density j, and n_e/n_0 are all functions of space within the plasma. Normalizing each of these quantities to its peak value gives

$$\langle n_e T_e\rangle = \frac{I\, n_e(0)\alpha^{1/2}}{T_e(0)^{1/4}}\, G \tag{13}$$

where I is the plasma current and G is a geometry factor depending on an integral over the profiles. This integral is defined by

$$G = \frac{1.4 \times 10^{-15}}{\pi a^2} \int_0^1 x dx\, \tilde{J}\left(\frac{1}{\tilde{T}_e}\right)^{1/4} \left(\frac{\tilde{\alpha}}{n_0 n_e}\right)^{1/2} \tag{14}$$

Where

$$\tilde{A} \equiv A(r)/A(0) \ .$$

We might expect this geometry factor G to be approximately constant since the first term in the integrand is the normalized current density whose integral over the cross section of the plasma equals a constant and since the remainder of the integrand is seen to be a slowly varying function. The unnormalized product of neutral density and electron density $n_0 \times n_e$ has been left in the geometry factor. This is done because experimentally we have observed that this product is approximately constant. The theoretical model and the experimental data which support this conclusion are given in the appendix.

Dividing the plasma energy content given by Equation 13 by the poloidal magnetic energy density at the limiter gives an expression for beta poloidal:

$$\beta_p = G \frac{n_e}{I} \frac{\alpha^{1/2}}{T_e^{1/4}} \tag{15}$$

Notice that the β_p obtained here does not depend on c the numerical coefficient of the pseudoclassical diffusion coefficient. Thus we see that the dominance of energy loss by particle diffusion over pseudoclassical electron thermal conductivity loss leads to a beta poloidal which is a function of the plasma parameters rather than a constant value. Also the particular functional form of D_{pc} given in Equation 5 is not necessary to produce the particular parametric dependence of β_p seen in the experiments summarized in Fig. 4.

There are, however, other consequences of the dominance of particle diffusion which do reflect the functional form of D_{pc} given in Equation 5. Since we are assuming that the electron energy is carried out by particles and since these particles must be replaced in the steady state we conclude that the plasma energy containment time is given by the particle ionization rate:

$$\tau_E = \tau_p = \frac{1}{n_0 \langle \sigma_i v_e \rangle} \tag{16}$$

Now since we have shown in the appendix that the neutral density in the central region of the plasma has a dependence

$$n_0(0) \propto \frac{n_0(a)}{n_e(0)} , \tag{17}$$

we conclude that the energy containment time in the plasma should be proportional to the electron density

$$\langle \tau_E \rangle \propto \langle n_e \rangle \ . \tag{18}$$

Now using our definition of the density scale length r_n we can write an equation for the electron density gradient in terms of the plasma parameters:

$$- \frac{\partial n_e}{\partial r} = + \frac{n_e}{r_n} = + n_e \sqrt{\frac{n_0 \langle \sigma_i v_e \rangle}{D_{pc}}} \tag{19}$$

Integrating this equation from the plasma surface to its center gives the dependence of the plasma electron density on the plasma parameters. This dependence is

$$n_e(0) \propto I \frac{T_e^{1/4}}{\alpha^{1/2}} \tag{20}$$

Then combining Equation 18 and Equation 20 we are led to the conclusion that the plasma energy containment time should be roughly proportional to the plasma current with a weaker dependence on the temperature and the anomaly factor

$$\langle \tau_E \rangle \ \alpha I \frac{T_e^{1/4}}{\alpha^{1/2}} \tag{21}$$

To summarize, a simple analysis of the electron energy balance when it is dominated by pseudoclassical particle diffusion gives the scalings

$$\beta_p = G \frac{n_e}{I} \frac{\alpha^{1/2}}{T_e^{1/4}} \qquad \text{(a)}$$

$$\tau_E \propto n_e \frac{T_e^{1/4}}{\alpha^{1/2}} \qquad \text{(b)} \qquad (22)$$

$$n_e \propto I \qquad \text{(c)}$$

where 22(b) and (c) hold at constant surface neutral density. All of these effects are in fact seen experimentally. A comparison of the data from the ORMAK experiment with the scaling indicated by Equation 22a is shown in Figure 6. The experimental data can be fit with only a 25% variation in the geometry factor. A further check on the scaling shown in Equation 22a can be obtained by using our plasma simulation computer code. Figure 7 shows the results of such a calculation. The external neutral density was fixed and the plasma current was varied. The figure shows the value of beta poloidal obtained for currents ranging between 60 and 160 kiloamperes plotted as a function of the scaling parameters of Equation 22a. The expected linear relation is evident. In this calculation the anomaly factor alpha was assumed to originate from the presence of impurity ions in the plasma and we assumed that the effective Z of these impurities was a constant.

Figure 8(a) shows data taken on the T-4 experiment under conditions in which the current flowing in the plasma was held constant and the density was varied by changing the initial gas filling. The linear relationship between the energy containment time and the average plasma

density predicted by Equation 22(b) is evident. In these experiments the resistivity anomaly factor was observed to vary approximately as $1/n_e$ and the electron temperature varied approximately as $1/n_e^{1/2}$. With these dependences included in Equation 22(a), we would expect the β_p to vary approximately as n_e. The experimentally measured β_p is in agreement with this expectation and is shown in Fig. 8(b).

The relationship predicted by Equation 22c is compared with experiment in Figure 9. From the figure we can see that the density is proportional to current if the external neutral pressure is maintained approximately constant. Deviations from this linear relationship are noted when the external pressure is varied. As mentioned in the appendix, our neutral particle measurements indicate a linear relationship between the neutral density outside the plasma during a discharge and the initial filling pressure p_0. Thus we interpret the data in Figure 6 to mean that the electron density is proportional to the current in the plasma when the external neutral density is maintained constant. Since the proportionality between the plasma density and the plasma current is derived using the functional form of pseudoclassical particle diffusion given by Eq. 10, this data constitutes experimental evidence for pseudoclassical particle diffusion.

Figure 10 shows the relationship between the gross energy containment measured on various experiments[8,9,10,11] and the current in those experiments. There is a rough linear relationship between these qualities as predicted by the combination of Equations 22(b) and (c).

The large scatter of points about the line, τ_e proportional to I, reflects the occurrence of several phenomena which are not reflected in

the simple scaling given by Equation 22. First, among these is the fact that in the experiments the surface density of neutral particles is not controlled. Secondly, as the current in an experiment is varied, the resistivity anomaly coefficient is observed to change.[14] This can be due either to a variation of the impurity content in the discharge or to the occurrence of microscopic turbulence[15] which increases the electron scattering rate although specific mechanisms for the generation of this turbulence are lacking.[16] The third phenomenon depends somewhat on the first two. This is the contribution of the electron thermal conductivity to the loss of energy from the plasma. As the neutral density and the anomalous resistivity in the discharge vary with current, the electron temperature profile will itself begin to vary and consequently the amount of energy flowing through the electron thermal conductivity channel will be a function of the plasma current. The physical argument leading to the scaling shown in Equation 22 is based on the assumption that particle diffusion is always the dominant energy loss mechanism. The computer simulation of the plasma operation shows that this is not entirely correct and we would expect some variation from the linear relationship between energy containment time and current such as is shown in Figure 10. In general, however, the simple scaling law based on the dominance of pseudo-classical particle diffusion seems to reflect the gross trend of the experiments. The individual points shown in Figure 7 can be reproduced by the computer simulations which do include the effect of electron thermal conductivity and an anomaly factor determined by the resistivity anomaly in that particular experiment. The scaling of n_e and τ_e with current obtained from these computer simulation calculations is shown in

Figure 11. In these simulation calculations the resistivity anomaly was taken to be due to the presence of impurity ions and was thus fixed as current was varied. The neutral density external to the simulated plasma was also taken to be fixed. Under these idealized circumstances the scaling of τ_e and n_e is in agreement with that predicted by Equation 22 and suggested by the data shown in Figures 6 and 7.

As a summary to this consideration of electron transport and scaling in Tokamaks, we can state that both the gross scaling of the plasma parameters and their quantitative values in particular experiments can be understood in terms of electron heat conduction and particle diffusion governed by pseudoclassical transport if one takes into account the variation of plasma resistance and neutral particle density in the experiments. We do not have any experimental evidence as to the nature of the process responsible for pseudoclassical diffusion nor do we completely understand the origin of the plasma resistivity anomaly. The former may be due to drift wave turbulence as suggested by Yoshikawa and the latter may be partially explained by the presence of impurity ions in the discharge.[17] Certainly further work is necessary to increase our understanding of these phenomena.

III. ION ENERGY BALANCE

Let us now turn to a consideration of the ion energy balance in the plasma. As in the case of the electron energy balance, Academician Artsimovich provided us with a fundamental insight which aided in a simple

conceptualization of the problem. He noted[18] that for the range of parameters ordinarily encountered in Tokamak discharges, the energy flow from the electrons to the ions, Q_{ei},

$$Q_{ei} = 3 \frac{m}{M} n\nu_{ei}(T_e - T_i) \tag{23}$$

could be simplified to

$$Q_{ei} \propto \frac{n_e^2}{T_i^{1/2}} \tag{24}$$

so that it depended only on the electron density and the ion temperature. This energy input to the ions is balanced by the loss processes of charge exchange, particle diffusion and ion heat conductivity. The first of these loss processes, Q_{cx}, can be roughly written as[19]

$$Q_{ex} \simeq n_0 n_i \overline{\sigma_{cx} v} T_i \tag{25}$$

If we were to equate this energy loss to the energy input from the electrons as written in Equation 24, we would find that the expected ion temperature depends only on the ratio of electron density to neutral density as shown in Equation 26.

$$T_i \propto (n_e/n_0)^{1/2} \tag{26}$$

This quantity n_e/n_0 has been given the name plasma quality by those working on target plasmas because it is a measure of the neutral shielding property of the plasma.

The next energy loss process for the plasma ions is by particle diffusion, which is described by

$$Q_D = \vec{\nabla} \cdot T_i D_{pc} \vec{\nabla} n \tag{27}$$

As was the case with electron energy loss through particle diffusion, we can make use of the fact that in the steady state this particle loss must be balanced by a particle source. Therefore, we can replace Equation 27 by the approximate relation given in Equation 28.

$$Q_D \cong n_0 n_e \langle \sigma_i v_e \rangle T_i \tag{28}$$

If we equate this ion energy loss to the energy input from the electrons given by Equation 24, we find that, as in the charge exchange dominated case, the ion temperature attained depends only on the plasma quality:

$$T_i \propto (n_e/n_0)^{2/3} \tag{29}$$

Therefore, we see that if charge exchange and particle diffusion were the only energy loss processes for the plasma ions the ion temperature attained would depend only on the plasma quality variable.

The third ion energy loss process is ion heat conductivity. This loss obeys Equation 30

$$Q_T = \nabla \cdot n_i \kappa_i \nabla T_i \tag{30}$$

where κ_i represents the ion thermal conductivity coefficient. The object of experiments on the ion energy balance is to determine the form of this thermal conductivity coefficient. The theoretical prediction of the form of κ_i has gone through an evolutionary process in recent years. This is summarized schematically in Figure 12. A calculation of ion heat conductivity in the absence of toroidal effects gives an ion heat conductivity

proportional to the ion collision frequency ν multiplied by the ion gyroradius squared. This is indicated by the dashed line in Figure 12. The inclusion of toroidal effects produces enhanced diffusion with a scaling that depends on the value of the collision frequency ν. In the collisional or Pfirsch-Schlüter[20] regime the classical heat conductivity is enhanced by the square of the inverse rotational transform q. At intermediate values of the collision frequency Galeev and Sagdeev[21] derived a heat conductivity which was independent of the collision frequency. At still lower values of the collision frequency[21] the heat conductivity was predicted to have a scaling similar to that in the Pfirsch-Schlüter regime enhanced by the 3/2 power of the inverse aspect ratio ε. The most recent calculation of the ion thermal conductivity by Hinton and Rosenbluth[22] spans the region between these two asymptotic regions.

The asymptotic form of the thermal conductivity coefficient predicted by the theory of Galeev and Sagdeev is shown by the upper dashed line in Figure 12. The correct form for the thermal conductivity coefficient in the intermediate range of collision frequency between the collisionless and the plateau regime obtained by Hinton and Rosenbluth[22] is shown schematically by the solid line in Figure 12. Tokamak experiments operate in the range of collision frequency between the collisionless and the plateau regime and therefore the theory of Hinton and Rosenbluth is the appropriate theory to use in describing these experiments. However, when Academician Artsimovich first considered the problem of ion energy balance in Tokamaks he had available to him only the theory of Galeev and Sagdeev. Using this theoretical expression for κ_i and replacing the gradient operators in Equation 30 by a scale length

he obtained an expresssion for the ion thermal conductivity loss Q_T. Equating this loss to Q_{ei} gave an expression for the ion temperature scaling in the experiment in the absence of particle diffusion and charge exchange. This scaling is

$$T_i \propto \sqrt[3]{n_e I} \text{ Galeev-Sagdeev} \tag{31}$$

Since the losses due to charge exchange and particle diffusion depend on the plasma quality it is justifiable to neglect these loss processes when the plasma quality is sufficiently high. However, the plasma quality is not large enough to justify this assumption in all regimes of Tokamak operation. Therefore we might expect deviations from the scaling indicated by Equation 31 as the plasma quality is varied. In addition, as is clear from Figure 10, the Galeev and Sagdeev expression for the ion thermal conductivity is larger than the more recent theory of Hinton and Rosenbluth would indicate. If we use the Hinton-Rosenbluth prediction of κ_i in Equation 30 we find in fact that the ion temperature is independent of electron density and depends on plasma current in the form

$$T_i \propto I^{2/3} \text{ Hinton-Rosenbluth} \tag{32}$$

For the range of collisionality[23] covered by the experiments, Figure 13 shows the scaling of ion temperature with plasma quality and current predicted by Equations 26, 29 and 32. Since Equation 32 does not depend explicitly on the plasma quality the thermal conductivity losses are indicated on the figure as ion heat conduction asymptotes. It is clear that no one loss process taken by itself is able to explain the observed ion temperatures. However, the sum of the three loss processes equated

to Q_{ei} gives a prediction for the ion temperature as a function of the plasma quality shown by the solid curves in Figure 13. There is reasonable agreement between these curves and the experimental data points.

We conclude from this agreement that the ion heat conductivity in the experiments is in reasonable agreement with the predictions of Hinton and Rosenbluth. On the other hand, Figure 14 shows ion temperature data obtained on the Russian experiments T-3 and T-4 plotted against the Artsimovich scaling parameter indicated in Equation 31.[24] Here we appear to have agreement between the data and the predictions of an archaic theory ignoring the effects of charge exchange and particle diffusion. The apparent contradiction between the models represented by Figure 13 and Figure 14 can be removed by recalling that the electron density is itself a function of the plasma current as shown in Figure 9 and Figure 11. If we, therefore, replace the density in Equation 31 by a constant times the current we see that the Artsimovich scaling gives a dependence of the ion temperature on current which is essentially the same as that obtained from the Hinton-Rosenbluth theory in Equation 32. Thus to the extent that $n_e \propto I$, Figure 14 shows, in effect, a plot of the ion temperature vs current to the 2/3 power which is exactly the dependence to be expected from the theory of Hinton and Rosenbluth. The data in Figure 13 also show this current dependence and in addition the dependence of the ion temperature on the plasma quality.

This interpretation of the relationship shown in Figure 14 can be confirmed with our pseudoclassical plasma simulation code. This code uses the Hinton-Rosenbluth form of the ion thermal conductivity. The ion temperatures obtained from this calculation are shown in Figure 15

as a function of the Artsimovich scaling parameters. The linear relationship obtained is just that found in the experimental data of Figure 14. Thus, we conclude that both the ORMAK experiment and the T-4 experiment produce ion temperatures which are consistent with the ion thermal heat conductivity as defined by Hinton and Rosenbluth.

IV. SUMMARY AND CONCLUSION

The general agreement between the experimentally observed plasma behavior in a variety of different Tokamaks and the predictions based on microscopic pseudoclassical and neo-classical diffusion coefficients can be taken as evidence that at least to the extent that the current theory of trapped particle instabilities[25] is valid, these theoretically predicted instabilities have not yet appeared in the experiment. The largest unknowns in our picture of the plasma behavior in Tokamaks are the mechanism producing pseudoclassical diffusion and the cause of the resistance anomaly, in so far as this anomaly cannot be attributed to the presence of impurity ions.

Appendix I

NEUTRAL PARTICLE BEHAVIOR IN TOKAMAKS

Although the density of neutral particles in Tokamaks is a small fraction of the plasma density, typically a few parts in 10^5, these particles are responsible for physical effects which greatly modify the behavior of the plasma. In order to understand the way in which neutral particles contribute to the dynamics of the plasma we must develop a theoretical model describing the behavior of the neutral particles themselves. The source of neutral particles is the wall bounding the plasma. This wall can emit neutral particles chemically adsorbed in the period before the creation of the plasma. It can also emit neutral particles under the impact of the various types of radiation emanating from the plasma. If the neutrals emitted from the wall have energies such that their mean free path for absorption is small compared to a typical plasma dimension they will penetrate only a relatively thin surface of the plasma. However, because this thin surface layer contains plasma ions with some temperature T_i, those neutrals that are absorbed by charge exchange give rise to a second generation of neutrals with energies characteristic of the surface ion temperature. These neutrals typically penetrate farther into the plasma than the colder, first generation neutrals. Subsequent charge exchange reactions with even more energetic ions in the interior of the plasma produce faster neutrals.

This process is schematically outlined in Figure A1. On the left of the Figure we show the wall emitting neutral hydrogen atoms and molecules. The hydrogen molecules are stopped by ionization in a few millimeters of the plasma. Because the H_2^+ ion carries a certain amount of

vibrational energy the neutral atoms produced by dissociate ionization have energies ranging from 1 to 10 eV.[26] The neutral hydrogen coming from the wall can be produced by the reflection of charge exchange particles emitted from the plasma and consequently can also possess nonnegligible amounts of energy.[27] In either case, our model envisions a flux of moderately energetic H_0 entering the plasma. These warm neutrals with energies between 4 and 30 eV produce second generation neutrals by charge exchange. A solution of the neutral transport equation shows that these secondary neutrals have mean energies typically 1/6 of the local ion temperature.

The Boltzmann equation given in the Figure describes the evolution of the energetic neutral distribution function f_0. The integral term in this equation describes the interchange of particles between the plasma ion distribution function and the neutral distribution function. The second term describes the loss of fast neutrals due to ionization by plasma electrons. The third term describes the source of fast neutral particles due to the influx of the first generation neutrals from the plasma surface. For reasons which will become clear we have assumed that these first generation neutrals are produced by the dissociative ionization of H_2^+ ions which result from the influx of H_2 molecules. This dissociative ionization process is frequently referred to as Frank-Condon dissociation and the neutrals resulting from this dissociation as Frank-Condon neutrals. The results of our neutral particle transport calculation will be found to be insensitive to this choice of a particular model describing the origin of the first generation neutrals.[28]

The transport equation shown in the Figure can be solved analytically by making certain simplifying assumptions. A more accurate solution which includes the spatially varying electron density and ion temperature of the plasma can be obtained numerically. An approximate solution[29] for the neutral density at the center of the plasma shows that this central neutral density has the characteristic form shown in the Figure. There are three dominant dependences which are most evident. The central neutral density is proportional to surface density of Frank-Condon neutrals. Secondly, the central neutral density is inversely proportional to the plasma electron density. And thirdly, the central neutral density is related in an exponential manner to an average plasma scale length divided by a mean free path for adsorption. The first two dependences result from the fact that the central neutral density is proportional to the number of neutrals in, and the thickness of, the surface layer which is the ultimate source of all neutrals in the plasma. The thickness of this surface layer is inversely proportional to the electron density; hence the $1/n_e$ dependence. The exponential factor is a reflection of the fact that neutrals originating in this surface layer are attenuated on their way to the plasma center. The exact numerical solution of the neutral transport problem which includes the self-consistent electron density and ion temperature profile gives the result that the Franck-Condon density N_{fc} times the attenuation factor is approximately constant over the range of plasma operation in the ORMAK device. Consequently, the neutral density in the plasma core is roughly given by $1/n_e$. The experimental data illustrating this behavior is shown in Figure A2.

The solid lines in the Figure show the result of a numerical solution of our transport equation. These lines indicate the ratio of the central neutral density normalized to the surface Frank-Condon neutral density as a function of the plasma electron density for different values of the plasma ion temperature. These curves are obtained using typical electron density and ion temperature radial profiles. The experimental data shown in the Figure were obtained by measuring the charge exchange flux Γ_{cx} emerging from the surface of the plasma as indicated in Figure A1.

This neutral flux was energy-analyzed in a neutral particle spectrometer. The number of neutral particles detected in each energy channel of the spectrometer was matched to that predicted by our numerical solution of the neutral particle transport equation using the experimentally determined electron density profile, the central ion temperature determined from the slope of the measured neutral particle flux and an assumed ion temperature profile consistent with the predictions of our plasma simulation codes. The surface neutral particle density was varied until agreement was obtained between the measured counts in each channel and the numerically predicted result. This procedure results in a self-consistent neutral particle profile across the plasma. It is superior to the traditional method of estimating neutral particle density from the measurement of the neutral flux emerging from the surface of the plasma in that it automatically accounts for the attenuation of the neutrals produced in the center of the plasma as they travel from the center to the surface. The experimental points shown in Figure A2 can be very well fit by the relationship $n_0 \propto N_{fc}/n_e$ and the deviation from this simple relationship is due to the ion temperature dependence in the attenuation factor shown in Figure A1.

Figure A3 shows the central neutral density as a function of electron density obtained from our plasma simulation computer code. This code solves the complete set of transport equations for the plasma density, the electron temperature, and the ion temperature as a function of radius. It also produces a simultaneous solution of the neutral transport equation given in Figure A1. The solid line in the Figure shows the variation of the central neutral density with plasma electron density when the surface Frank-Condon density is maintained constant. The variation in n_e was produced by varying the total plasma current in the calculation. Since the pseudoclassical particle diffusion coefficient, the pseudoclassical electron thermal diffusion coefficient and the neo-classical ion thermal diffusion coefficient were used in this computer simulation the solid line in Figure A3 represents the self-consistent neutral density variation to be expected in a pseudoclassical plasma. The dotted line represents the variation of the central neutral density predicted by the simple relation $n_0 n_e$ = a constant. All of the data shown can be fit with a relation of this type with only an 8% error over the range of densities shown. This is in substantial agreement with the variation of the experimental data shown in Figure A2.

Figure A4 shows a calculation of the energetic neutral density normalized to surface Frank-Condon density as a function of radius in the ST Tokamak. The variation shown in this Figure is typical of that seen in other Tokamaks. The various curves shown in the Figure illustrate the effect of impurity ions in the plasma on the profile of neutral hydrogen. From the second equation of Figure A1 we can see that impurity ions in the plasma will modify the neutral profile in two ways. First,

since the presence of an impurity ion implies the absence of a number of hydrogen ions equal to the impurities' charge, the contribution of charge exchange in the attenuation factor will be reduced. On the other hand, since the energetic neutrals are produced by a multiple resonant charge exchange process this reduction in the hydrogen ion density will decrease the production rate of energetic neutrals. The data shown in Figure A4 reflect these two competing effects. These data indicate that the balance is almost complete in the central region of the plasma in that the neutral density in this region is essentially unaffected by the presence of substantial numbers of impurities. However, the density of neutral atoms in the surface layers of the plasma is reduced by the presence of impurity ions in the plasma. Figure A5 illustrates the variation of the maximum and the central values of the hot neutral density with impurity concentration for the ST and the ORMAK experiments. The fact that the neutral density is insensitive to the fraction of impurities over a large portion of the plasma means that measurements of the central ion temperature and the central neutral density by charge exchange spectrometers are insensitive to the presence of impurities. Furthermore, the contribution of this neutral density to the energy loss from the central region of the plasma will be unaffected by the presence of impurities. On the other hand, since the hot neutral density in the surface layers of the plasma is quite strongly affected by the concentration of impurities the energy loss from the surface of the plasma by charge exchange will be significantly altered by the presence of impurities. In the ORMAK plasma calorimetric probe measurements indicate that the plasma energy, which flows to the surface by particle diffusion and heat

conduction, is transferred to the walls of the device mainly by radiation and charge exchange. Estimates[30] based on qualitative observations of limiter heating in the ST Tokamak suggest that, at least under certain conditions, the plasma energy is carried to the limiter by heat conduction and is not transferred to the walls by charge exchange and radiation. This difference might be explained by a larger surface impurity content in the ST Tokamak since an increase in impurities would reduce the charge exchange flux from the surface of the plasma and increase the diffusive energy transfer.

In comparing theoretical models of the effects of neutral particles on plasma behavior with experimental data, we are confronted by a difficulty in that there is no direct measurement of the surface density of neutral particles which provide the source of neutrals in the bulk of the plasma. All of these theoretical predictions, based on a neutral particle transport calculation, would be proportional to this surface neutral density which we have labeled N_{fc}. On the ORMAK experiment we have observed that the surface neutral density, required to match the predictions of our neutral transport calculations with the experimental data, which we shall term N_{fc}* has a definite relation to the filling pressure of the device. Let us define a surface neutral density, N_{fc}^{model}, in the following way:

$$N_{fc}^{model} = 8 \times 10^9 \ (p_0/3 \times 10^{-4}) \ cm^{-3} \qquad (A1)$$

where p_0 is the gauge pressure in torr. Equation A1 represents a relation between the surface neutral density and the initial filling pressure which fits the general trend of our experimental data. Figure A6 shows

the ratio of N_{fc}^{*} to N_{fc}^{model} as a function of filling pressure for the ORMAK experiment. The standard deviation from unity of the data shown is .1, showing a good statistical correlation between the surface neutral density required to fit our measurements and the initial filling pressure. Therefore, in general, we would expect experiments using a constant filling pressure to approximate the results predicted by computer models which fix the surface neutral density, although individual experiments may deviate from this expectation. The physical process of neutral production, which is suggested by the data shown in Figure A6 is an evolution of adsorbed gas from the wall of the chamber during the course of the discharge. Since the data points shown correspond to a plasma current variation from 60 to 170 kiloamperes this gas evolution appears to be relatively independent of the plasma energy content and, one would surmise, of the direct interaction of the plasma with the wall. Because of the equilibrium nature of this apparent gas evolution, we expect the hydrogen to be in the form of H_2 molecules and consequently we have chosen the Franck-Condon dissociation process as the source of our first generation neutrals rather than postulating a flux of warm hydrogen atoms from the wall.

No data similar to that shown in Figure A6 is available from other experiments, and it is quite possible that the particular dependence of the surface neutral density on filling pressure suggested by the data in Figure A6 is a relation peculiar to the ORMAK experiment. This could be because the ORMAK experiment was designed with gold-plated liner in contrast to the stainless steel liners employed in most other Tokamak experiments. This liner material was chosen because of its low chemical

activity with gases expected to be found in the experiment. As has also been observed on other Tokamaks,[31] approximately half of the gas initially contained within the liner is adsorbed on the wall of the device during the breakdown process. Thus there is ample gas on the wall to supply the necessary neutral flux to the surface of the plasma. It is quite reasonable to assume that the rate of this gas evolution from the wall would be a function of the chemical bonding between hydrogen and the particular wall material. Experiments or theoretical calculations to clarify this situation would be quite welcome since we have shown that the behavior of neutral particles in the plasma plays a very dominant role in the determination of the observable quantities in the plasma.

ACKNOWLEDGMENTS

The ORMAK data contained in this report were provided by M. Murakami and L. A. Berry. We are grateful for their efforts and those of the whole ORMAK Operation Group. The plasma simulation results were obtained from J. T. Hogan and his active participation in discussions which led to the models outlined in this report was crucial. As usual J. Callen proved to be an invaluable source of information on theoretical topics.

Discussions with H. P. Furth and S. Strelkov and others at PPPL and the Kurchatov Institute are also gratefully acknowledged.

REFERENCES

1. Dimock, D. L., et al., Nuc. Fus. 13, 271 (1973).
2. Artsimovich, L. A., JETP Letters 13, 70, 1971.
3. Anashin, A. M., et al., JETP 60, 2095, 1970.
4. Yoshikawa, S., and Christophilos, N. C., Plasma Physics and Controlled Nuclear Fusion Research, Madison (IAEA, Vienna, 1973) Vol. II.
5. Gorbunov, B. P., Mirnov, S. Z., Strelkov, V. S., Nuclear Fusion 10, 43, 1970.
6. Kelley, G. G., et al., III Int. Symp. on Toroidal Plasma Confinement, Garching, F. D. R. (1973).
7. Dnestrovskii, Y. H., and Kostomarov, D. P., Pavlova, N. L., IV Eur. Conf. on Contr. Fusion and Plasma Phys., Rome (1971).
8. Dimock, D. L., et al., Plasma Physics and Contr. Nucl. Fusion, Madison (IAEA, Vienna, 1971) Vol. I.
9. Anashin, A. M., et al., Sov. Phys. JETP 33, 1127 (1971).
10. Artsimovich, L. A., et al., Plasma Phys. and Contr. Fusion Research, Madison (IAEA, Vienna, 1972) Supplement.
11. Murakami, M., et al., to be published.
12. Ibid.
13. Dimock, D. L., op. cit.
14. Bobrovsky, G. A., Kuznetsov, E. I., Razumova, K. A., JETP 59, 1103 (1970).
15. Rudakov, L. I., Zavoisky, E. K., Atomic Energy 23, 417 (1967).
16. Callen, J. E., Hogan, J. T., and Waddell, B. V., Third Int. Symposium on Toroidal Plasma Confinement, Garching, March 26-30, 1973.

17. Stodiek, W., V. Eur. Conf. on Contr. Fusion and Plasma Phys., Grenoble (1972).

18. Artsimovich, L. A., Gorbunov, E. P., Petrov, M. P., JETP Letters 12, 89 (1970).

19. Sigmar, D. J., Clarke, J. F., Physics of Fluids (to be published).

20. Pfirsch, D., Schlüter, A., Report Max Planck Institute, Munich, MPI-PA 7, 62.

21. Galeev, A. A., Sagdeev, R. Z., JETP 53, 348 (1966).

22. Hinton, F. L., and Rosenbluth, M. N., Physics of Fluids 16, 936 (1973).

23. Berry, L. A., Hogan, J. T., Clarke, J. F., Phys. Rev. Letters (to be published).

24. Strelkov, et al., VI Eur. Conf. on Contr. Fusion and Plasma Physics, Moscow (July 1973).

25. Kadomtsev, B. B., and Pogutse, O. P., Nuclear Fusion 11, 67 (1971).

26. McDaniel, E. W., Collision Phenomena in Ionized Gases, J. Wiley and Sons, New York (1964).

27. Barnett, C. F. (private communication).

28. Rehker, S., and Wobig, H., VI Eur. Conf. on Contr. Fusion and Plasma Physics, Moscow (July 1973).

29. Hogan, J. T. (private communication).

30. Furth, H. P. (private communication).

31. Gorbunov, E. P., Kotel'nikov, Yu. N., Kutukov, G. P., Simonov, V. A., Tech. Physics 11, 1363 (1967).

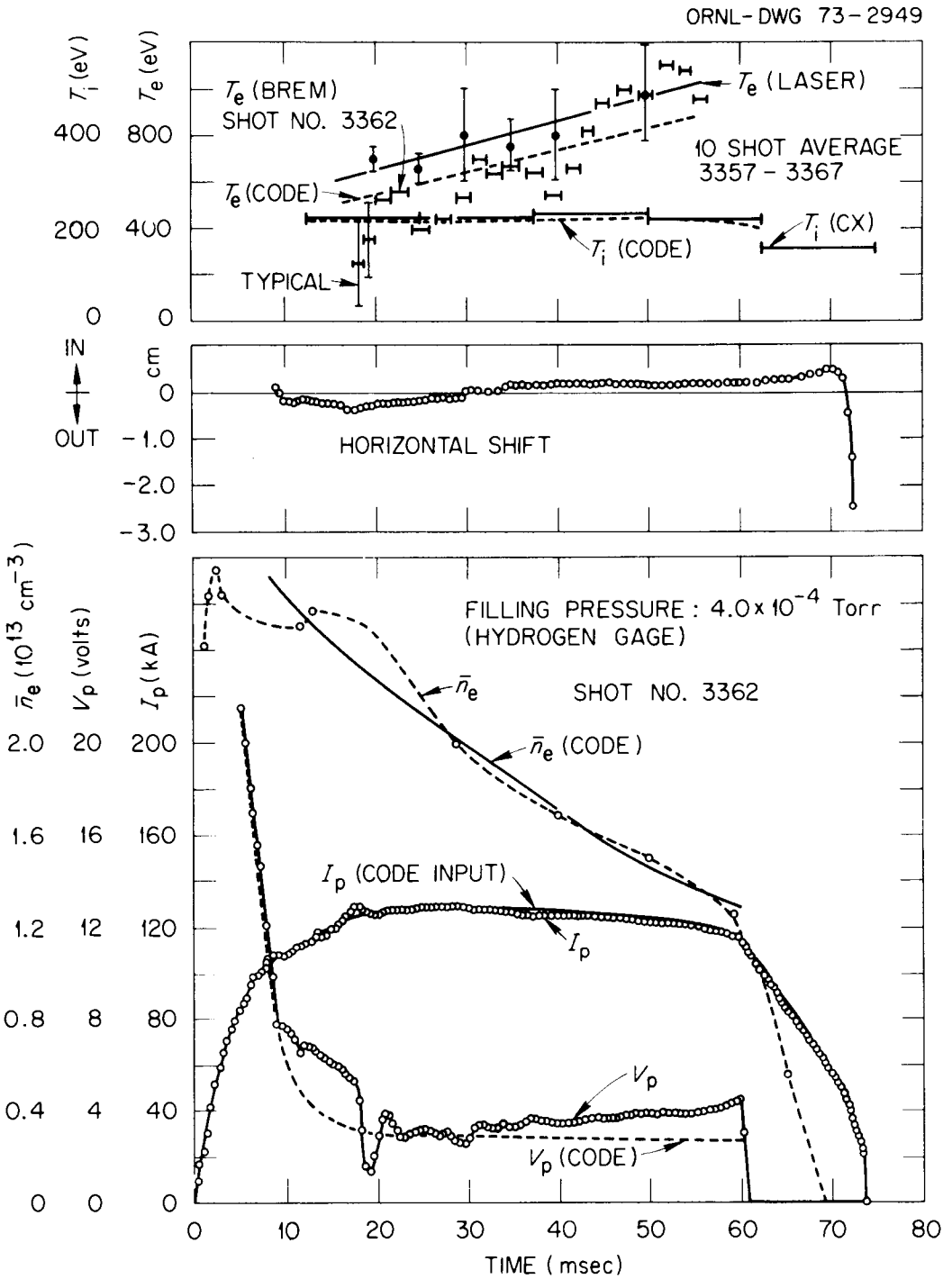

Fig. 1. The time behavior of the electron temperature, the ion temperature, the electron density, the horizontal plasma shift, and the voltage necessary to drive the programmed current for a particular ORMAK discharge is shown. The deviation of the predicted voltage from the measured voltage at the end of the discharge is an indication that the classical plasma resistivity with an effective Z of 3.5 was not adequate to describe the actual behavior of the plasma resistivity at late times. The fact that this discrepancy becomes more pronounced at the end of the discharge when the electron density has fallen to about half of its initial value reflects the well known $1/n_e$ dependence of plasma resistivity due to microturbulence observed on other Tokamak discharges.

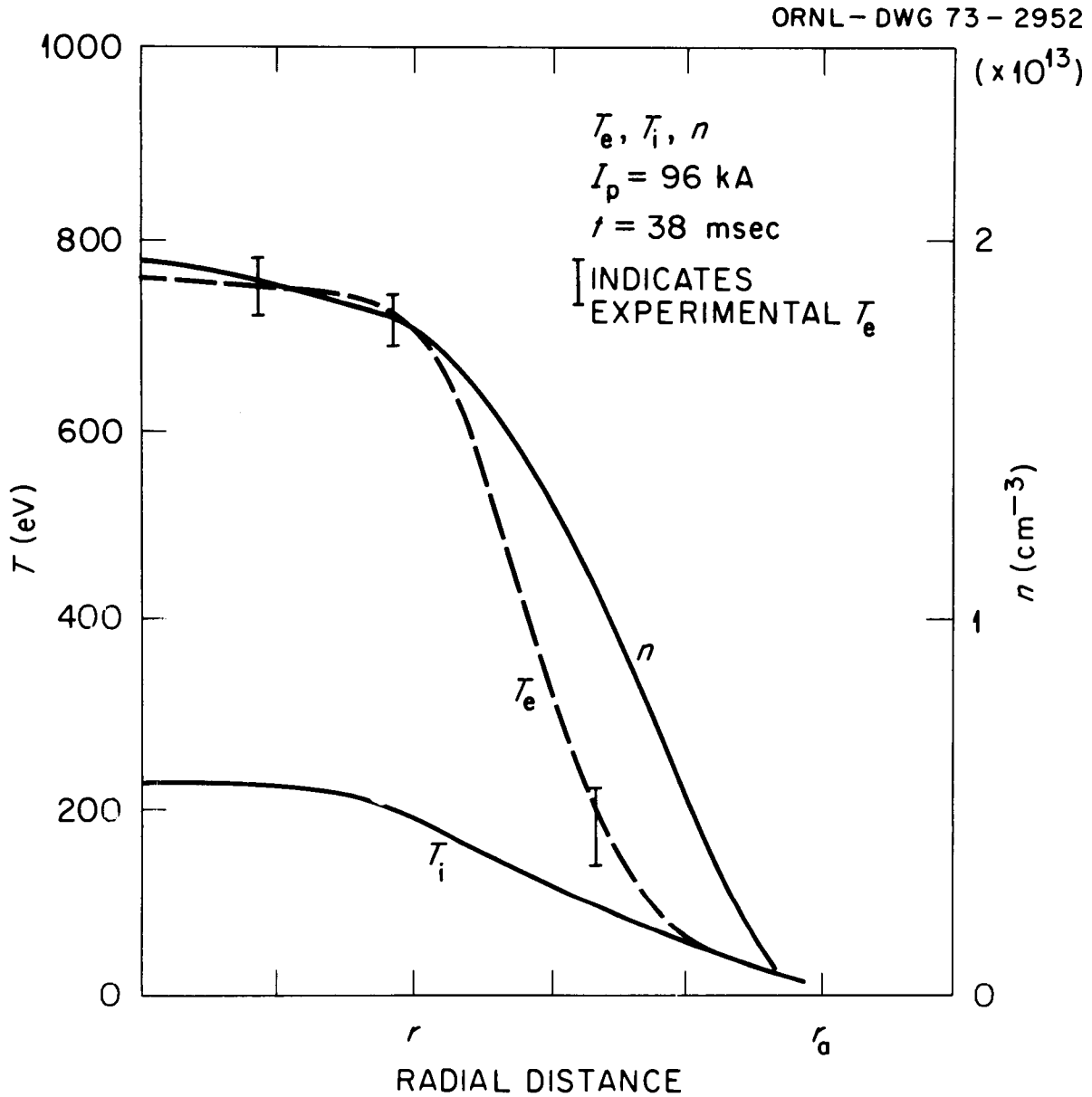

Fig. 2. Comparison of the predicted electron temperature and density and ion temperature profiles attained from a computer simulation calculation. The laser temperature measured at three radial positions is also shown.

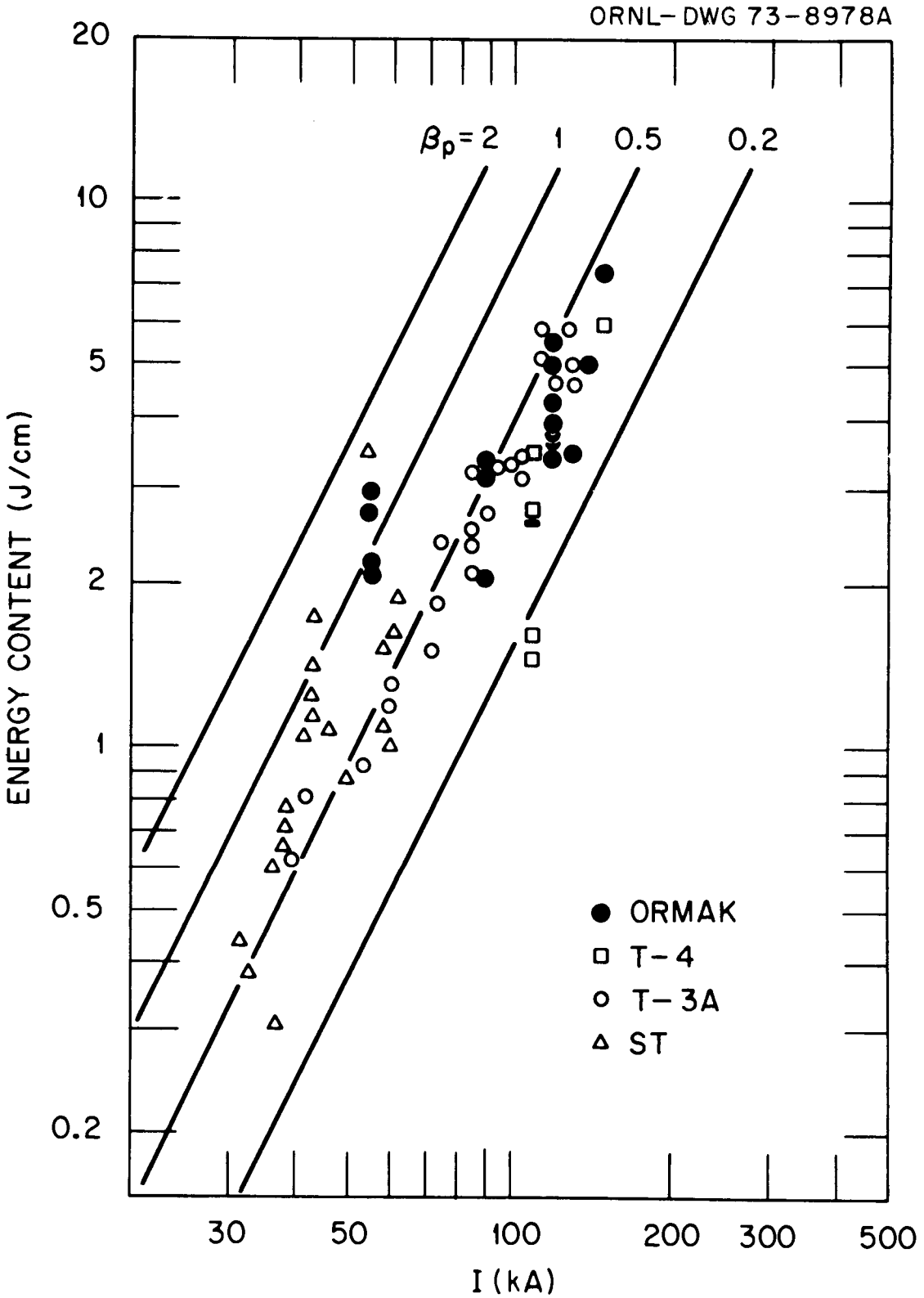

Fig. 3. The energy content of the plasma per unit length obtained on four Tokamak experiments as a function of the plasma current. The deviation of the data from the β_p constant lines is evident.

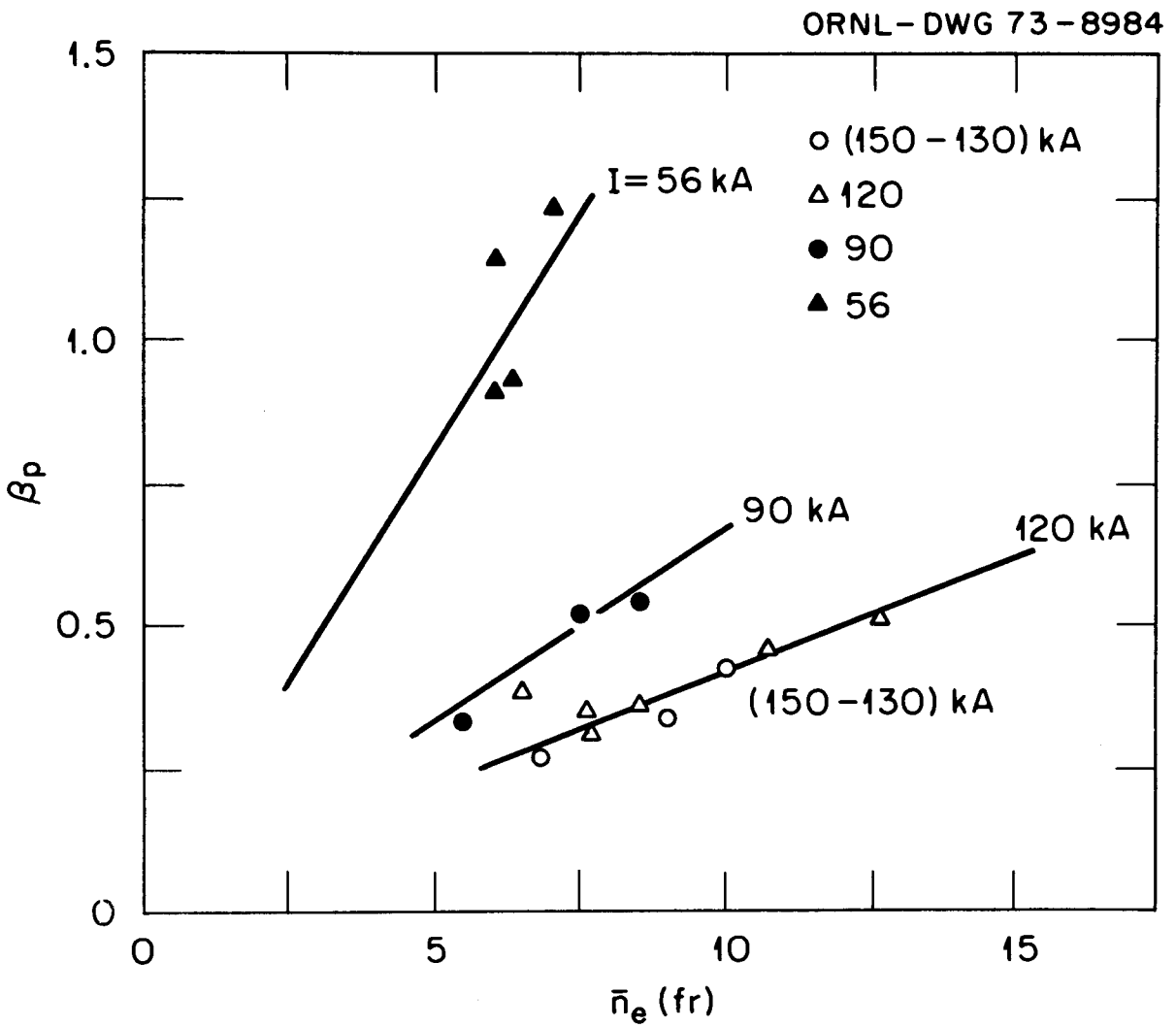

Fig. 4. The dependence of β_p on the electron density and plasma current in the ORMAK device.

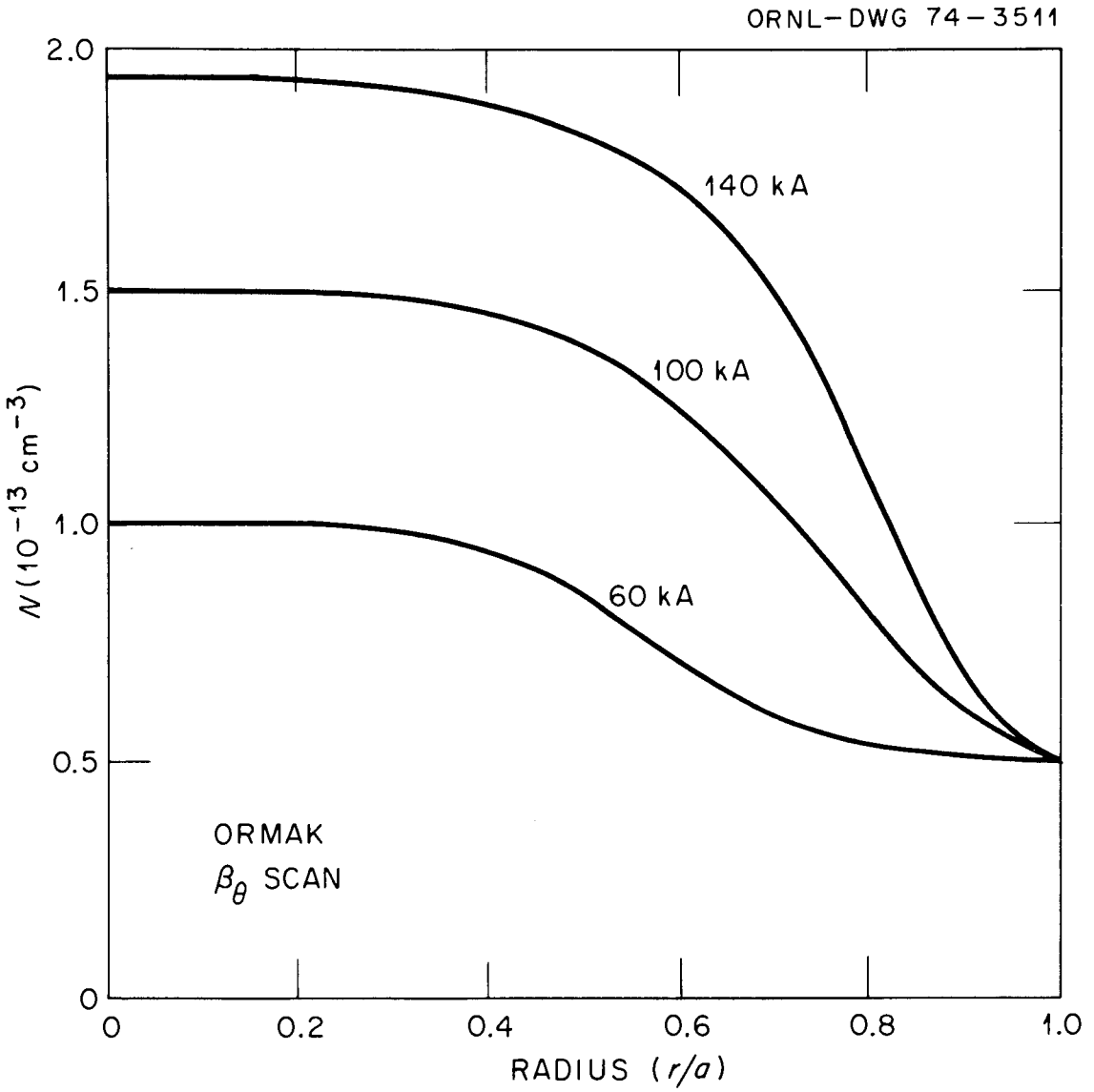

Fig. 5. The electron density obtained by computer simulation of the ORMAK plasma as a function of radius for several plasma currents. These profiles show a change in the density gradient as the current is varied.

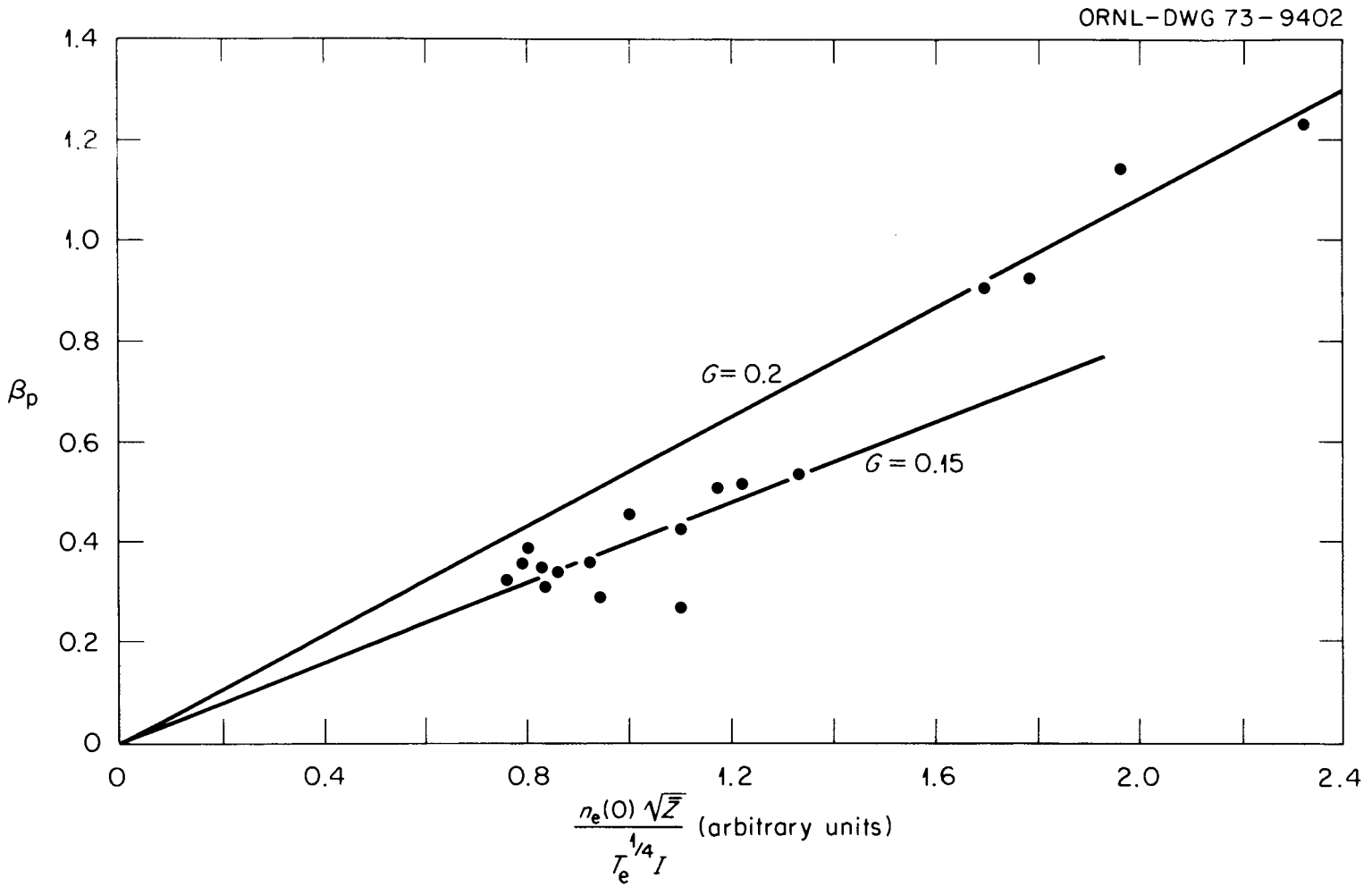

Fig. 6. The β_p predicted by the simple scaling which includes the variation of the electron density as a function of the scaling parameters. The experimental data shown in Figure 4 for 90, 120, and 130 through 150 kiloamperes can be fit with a geometry factor of .15. The 56 kiloampere data from Figure 4 can be fit with a geometry factor of .2.

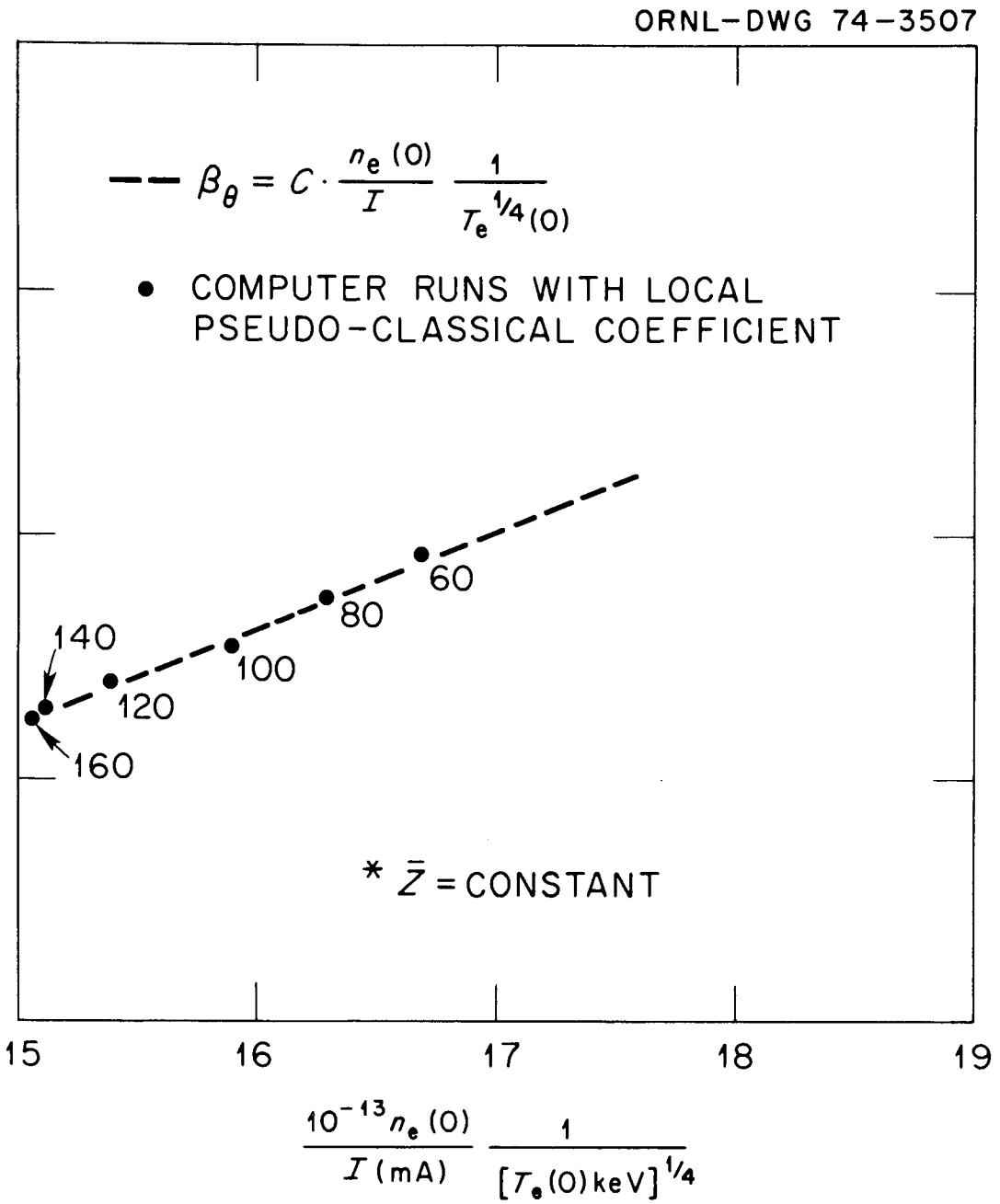

Fig. 7. The variation in β_p obtained from our plasma simulation code as a function of the scaling parameter of Equation 22a.

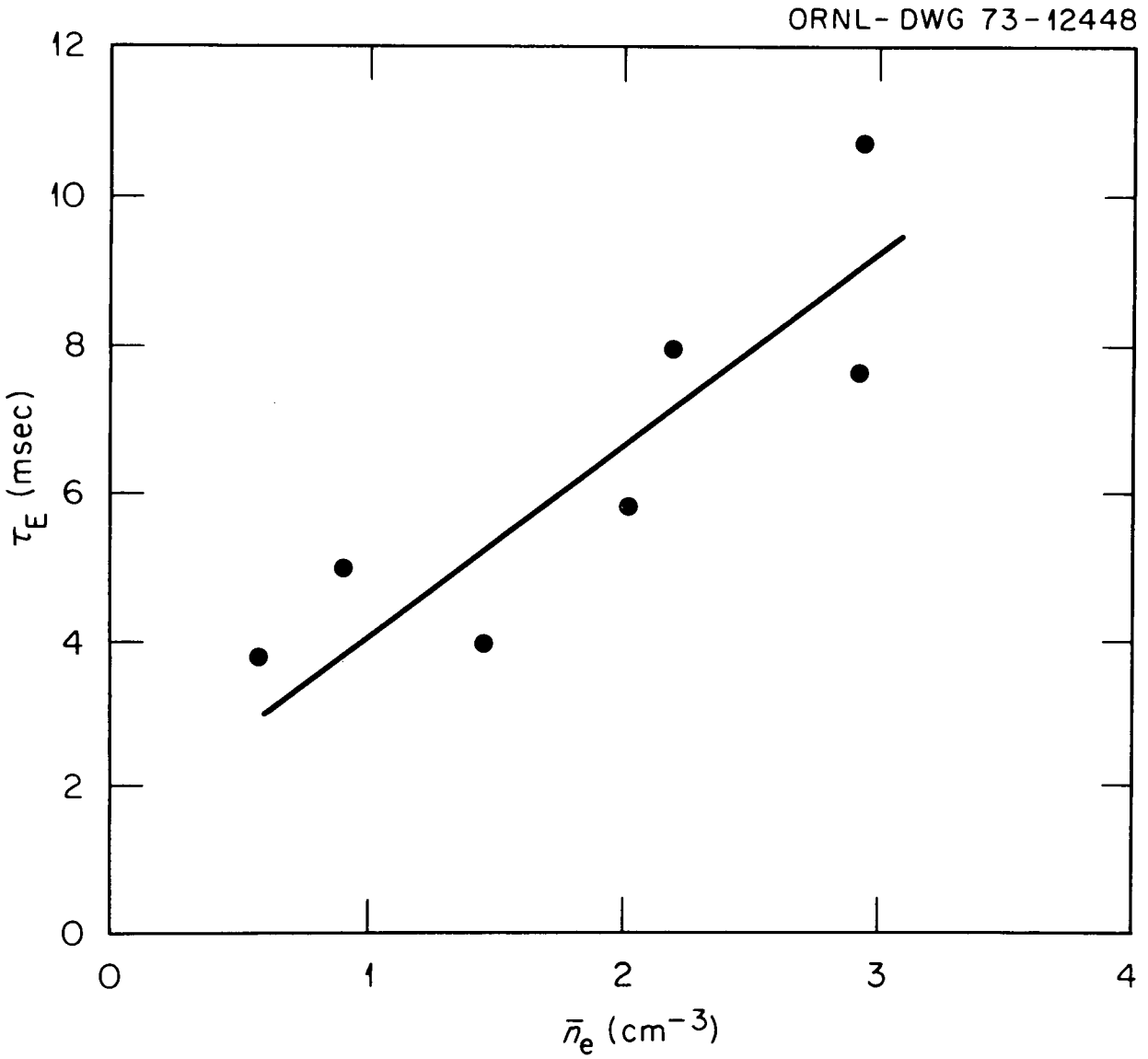

Fig. 8a. The energy containment time obtained on the T-4 experiment is shown as a function of the electron density. These data were obtained by fixing the plasma current and varying the filling pressure.

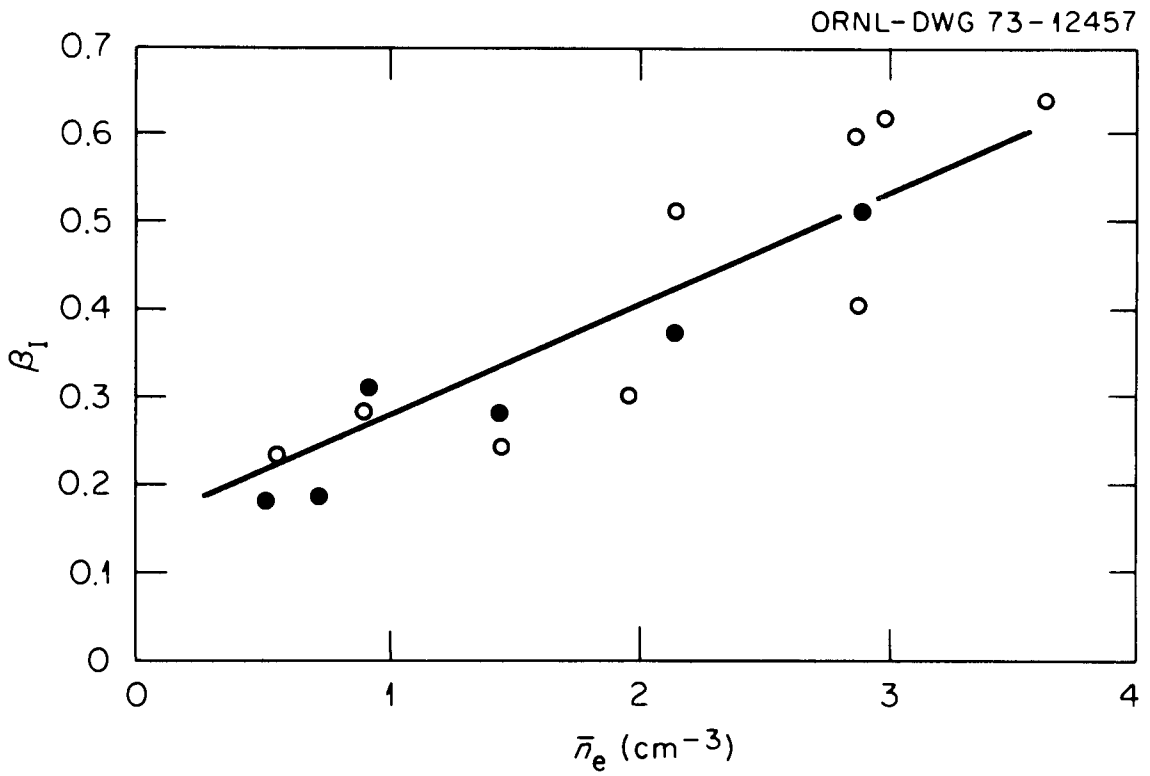

Fig. 8b. The β_p measured on the T-4 experiment is shown as a function of the density. The linear dependence shown follows from Equation 22a when the experimentally measured variation of the resistivity anomaly factor α is included.

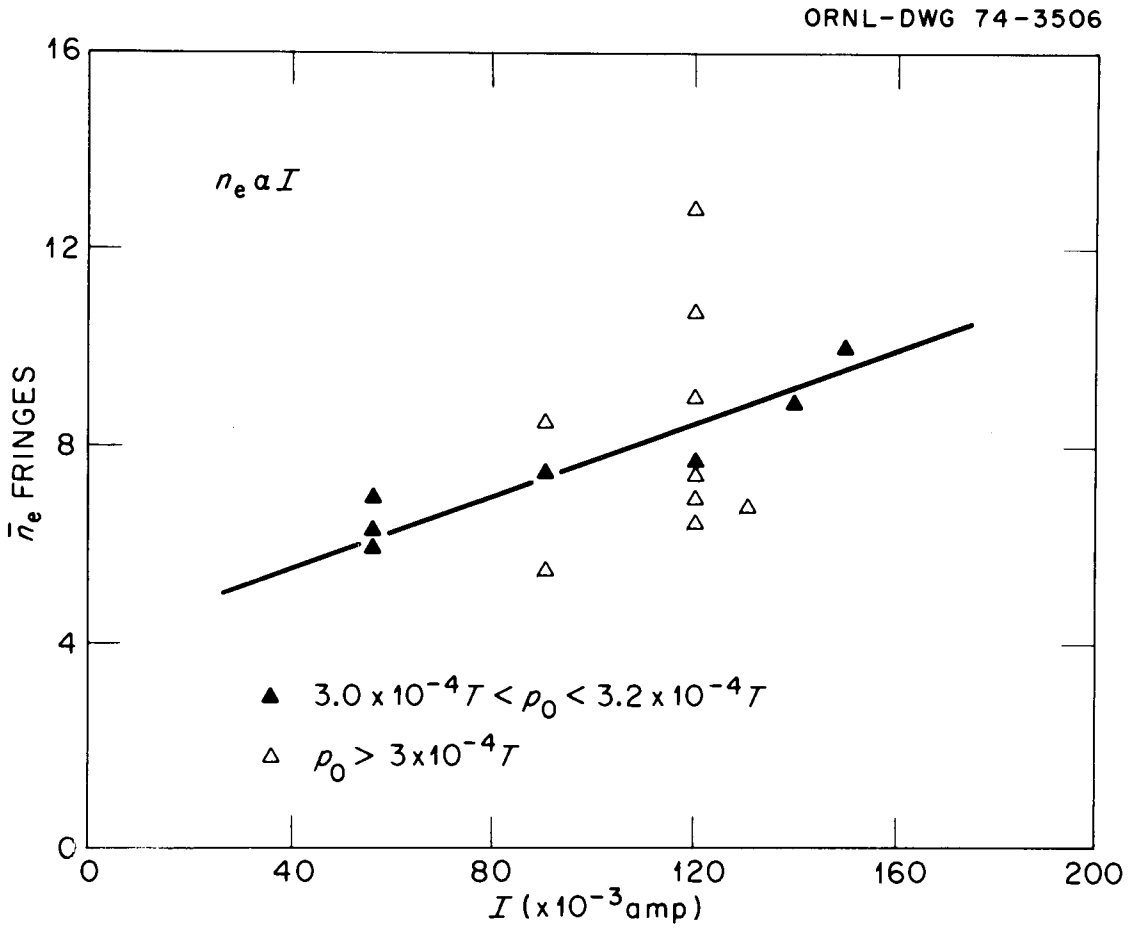

Fig. 9. The average electron density measured in terms of microwave interferometer fringes as a function of the plasma current in ORMAK. The expected linear relationship between the electron density and the current is evident in those experiments where the external pressure was maintained approximately constant.

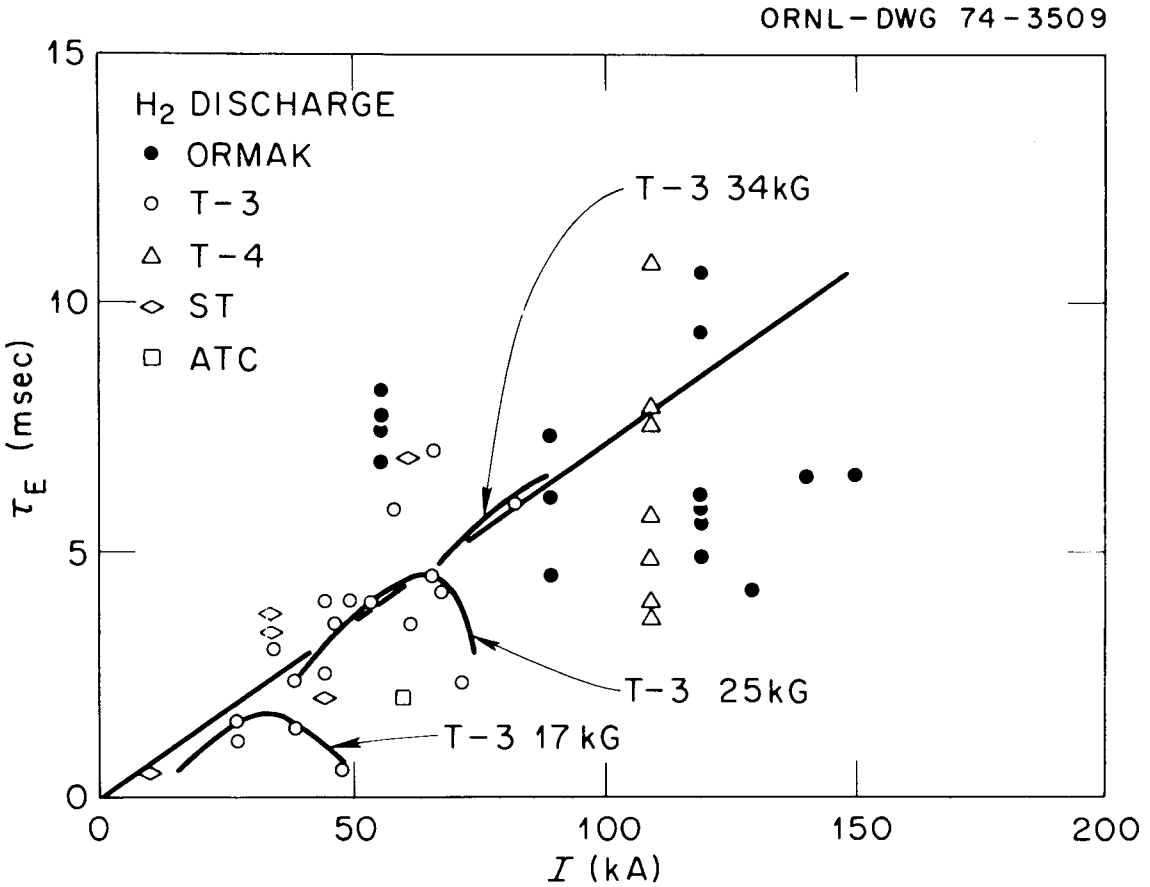

Fig. 10. The relationship between the experimentally determined gross energy containment time τ_E and the plasma current. The linear relationship predicted by Equation 22b and 22c is evident in the general trend of the data. An average of all of the data points at a given current would fall quite near the line. This general agreement is remarkable in that it is obtained for data from four different experiments operated under a variety of conditions of plasma purity.

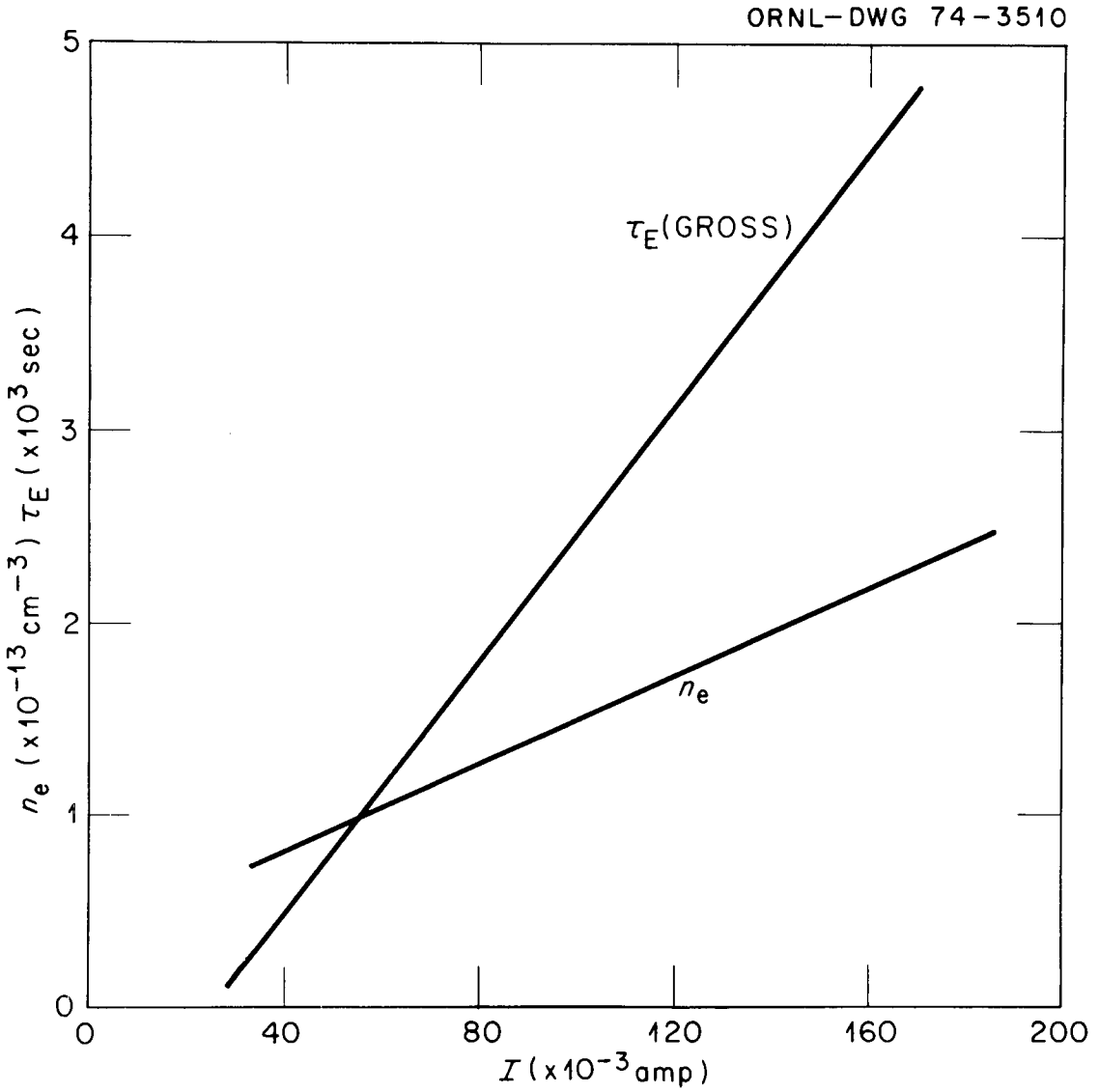

Fig. 11. The electron density and energy containment time obtained from our pseudoclassical plasma simulation calculation as a function of plasma current. Here the expected linear variation of both quantities is readily apparent.

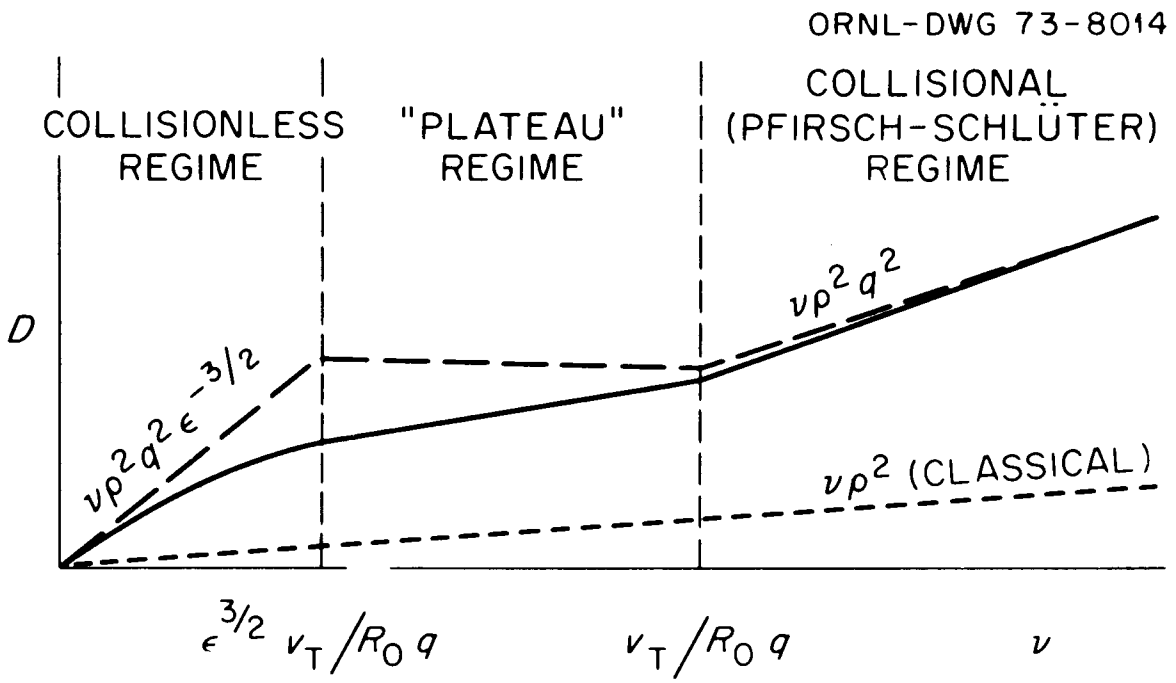

Fig. 12. The ion thermal conductivity coefficient κ_i is shown as a function of the effective collision frequency in the plasma. The upper dashed curve shows the dependence of κ_i on collision frequency predicted by Galeev and Sagdeev. The lower dashed curve shows the classical dependence. The intermediate curve is the dependence predicted by Hinton and Rosenbluth.

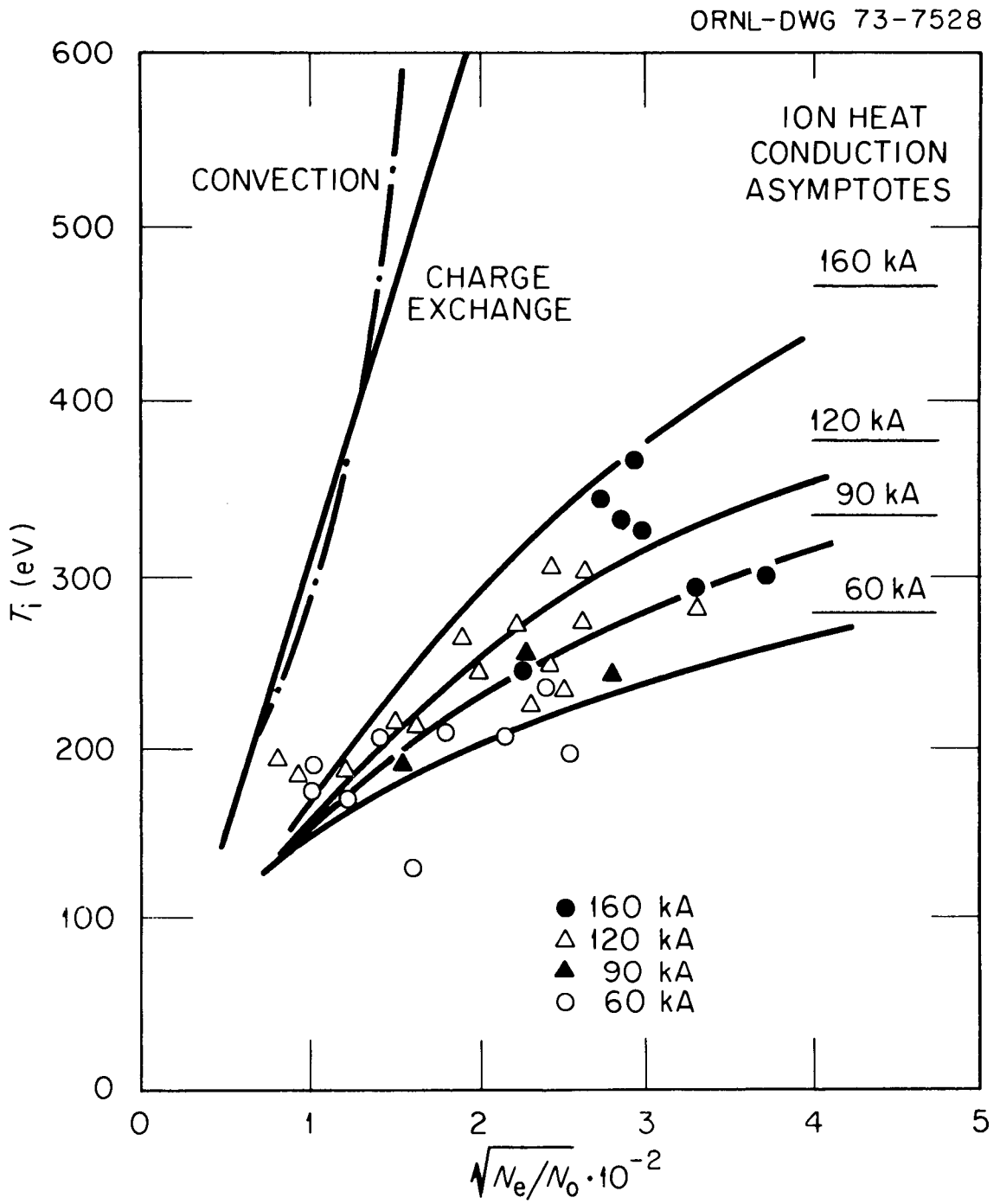

Fig. 13. The dependence of the plasma ion temperature on the plasma quality and plasma current. The experimental data agree with a theoretical model including losses by convection, charge exchange, and neo-classical ion heat conductivity.

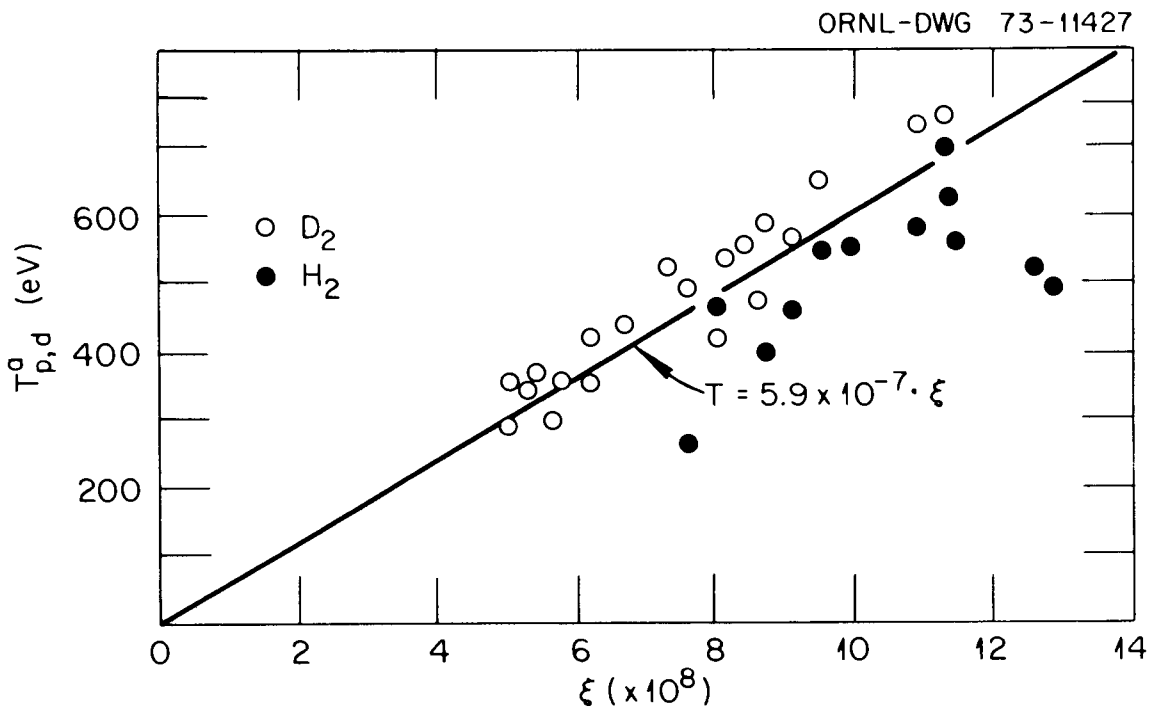

Fig. 14. The dependence of the ion temperature observed in the T3 and T4 experiments in terms of the parameter $\xi = 1/\sqrt{M} \cdot \sqrt[3]{In_e R^2 B_T}$. The ORMAK data of Figure 12 could also be plotted as a function of ξ and a similar linear relationship between T_i and ξ could also be inferred from this data.

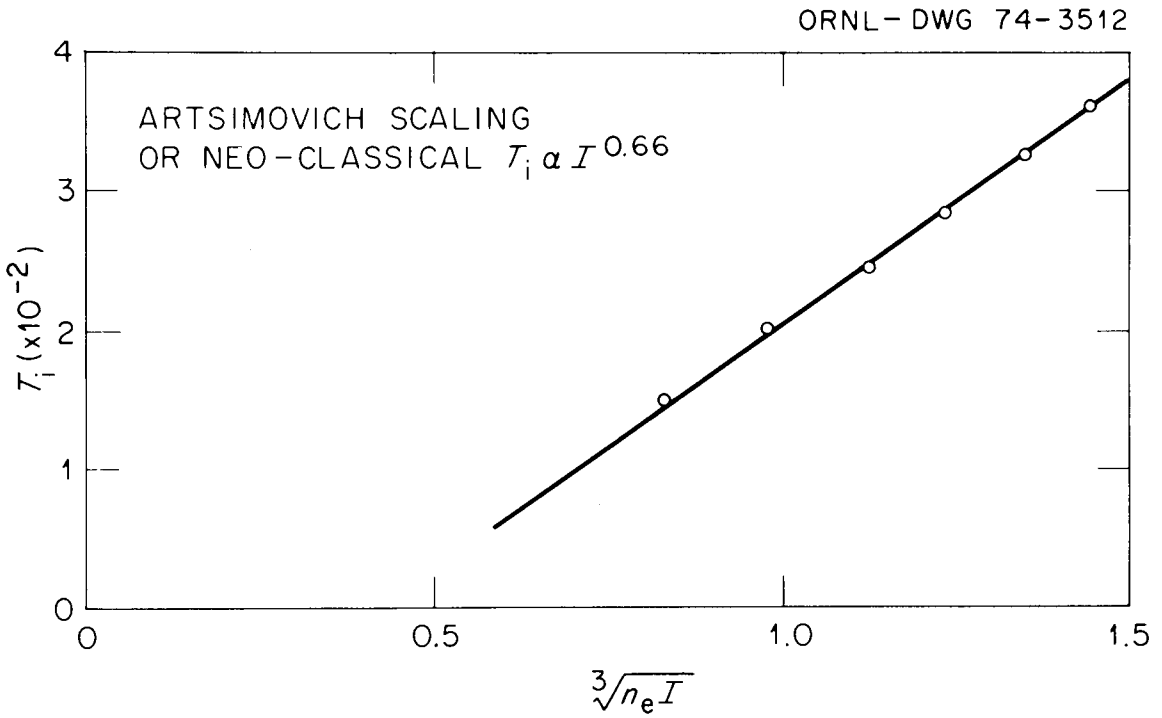

Fig. 15. The ion temperature obtained from our plasma simulation code which uses pseudoclassical electron transport coefficients and the Hinton-Rosenbluth neo-classical ion thermal conductivity as a function of $\sqrt[3]{n_e \times I}$. The linear dependence is similar to that seen in Figure 13.

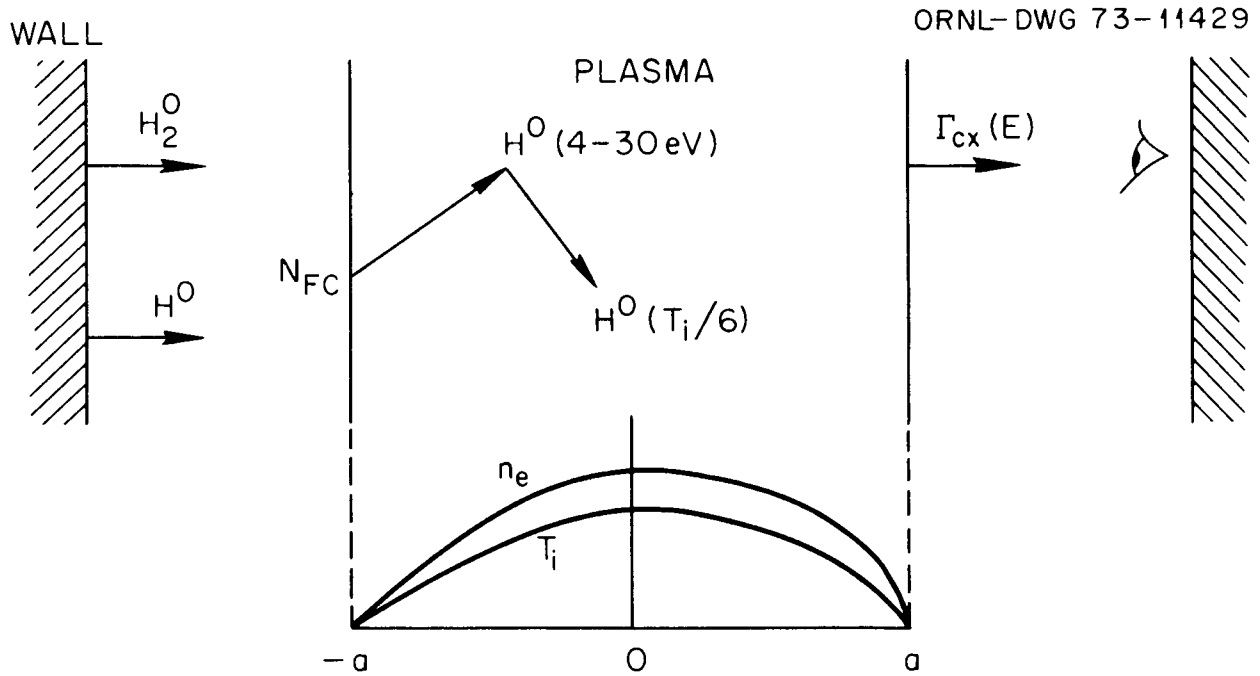

$$v_z \frac{\partial f_0}{\partial z} = \int dv^3 \; \sigma_{cx} \, |v - v'| \left[f_i(v) \, f_0(v') - f_i(v') \, f_0(v) \right]$$
$$- n_e(z) \; \langle \sigma_i \, v_e \rangle \; f_0$$
$$+ N_{FC}(z) \; \langle \sigma_{cx} \, v_i \rangle \; f_i$$

$$\text{FIND } n_0(0) \;\; \alpha \; \frac{N_{FC}}{n_e} \; e^{-\left\langle n_e \, a \left[\sigma_{cx} + \frac{\langle \sigma_i \, v_e \rangle}{v_i} \right] \right\rangle}$$

SURFACE LAYER

ATTENUATION ≃ CONSTANT

Fig. A1. The various elements of our neutral particle transport model are indicated in this Figure. The neutral particle transport is governed by the Boltzmann equation shown. An approximate solution of this Boltzmann equation gives the central neutral density scaling as shown at the bottom.

ORNL-DWG 73-7529

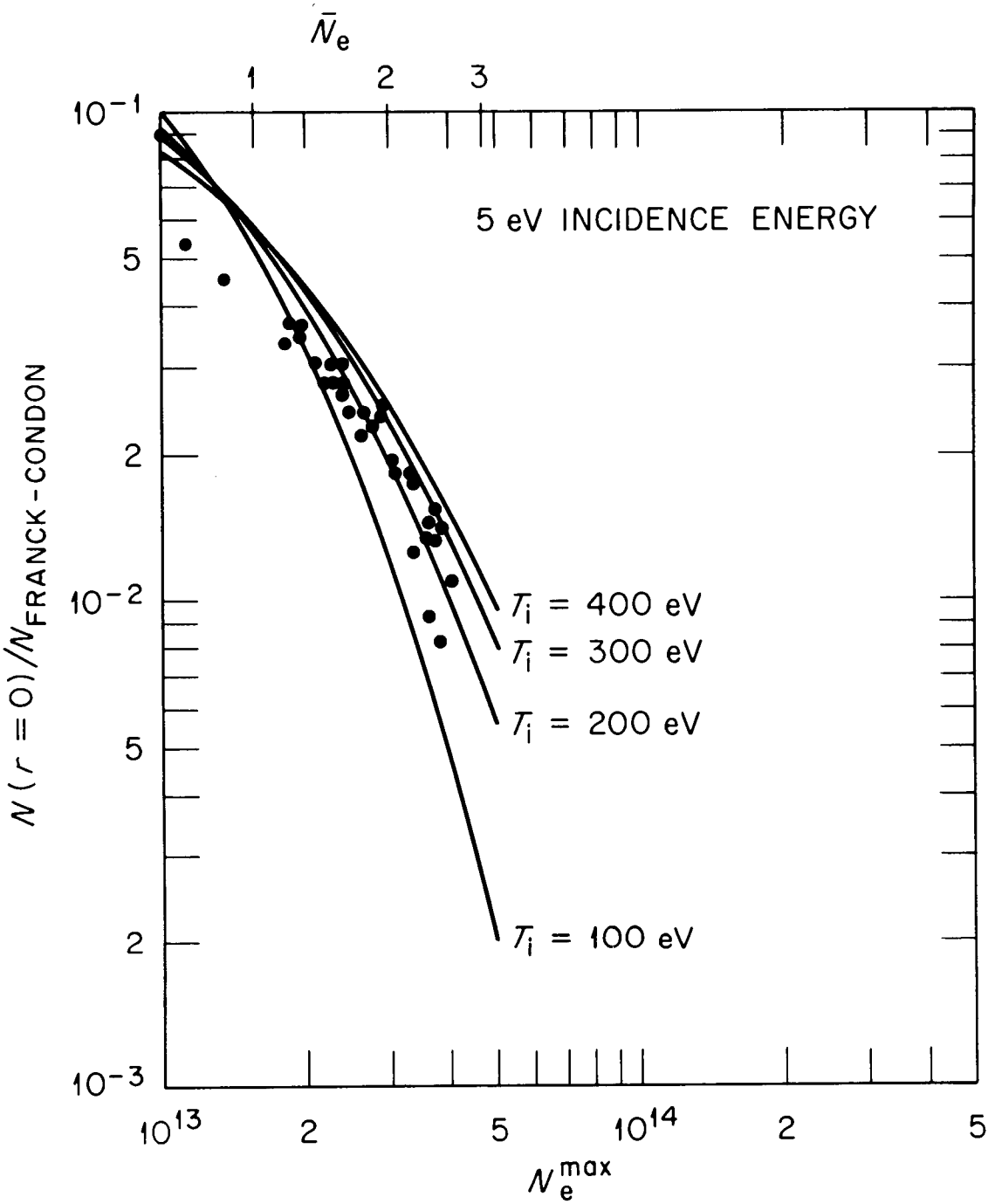

Fig. A2. The central neutral density, normalized to the surface Franck-Condon density, predicted by our neutral transport model as a function of the maximum electron density. The experimentally measured central neutral densities are also shown in the Figure in units of 3.6×10^{10} cm^{-3}.

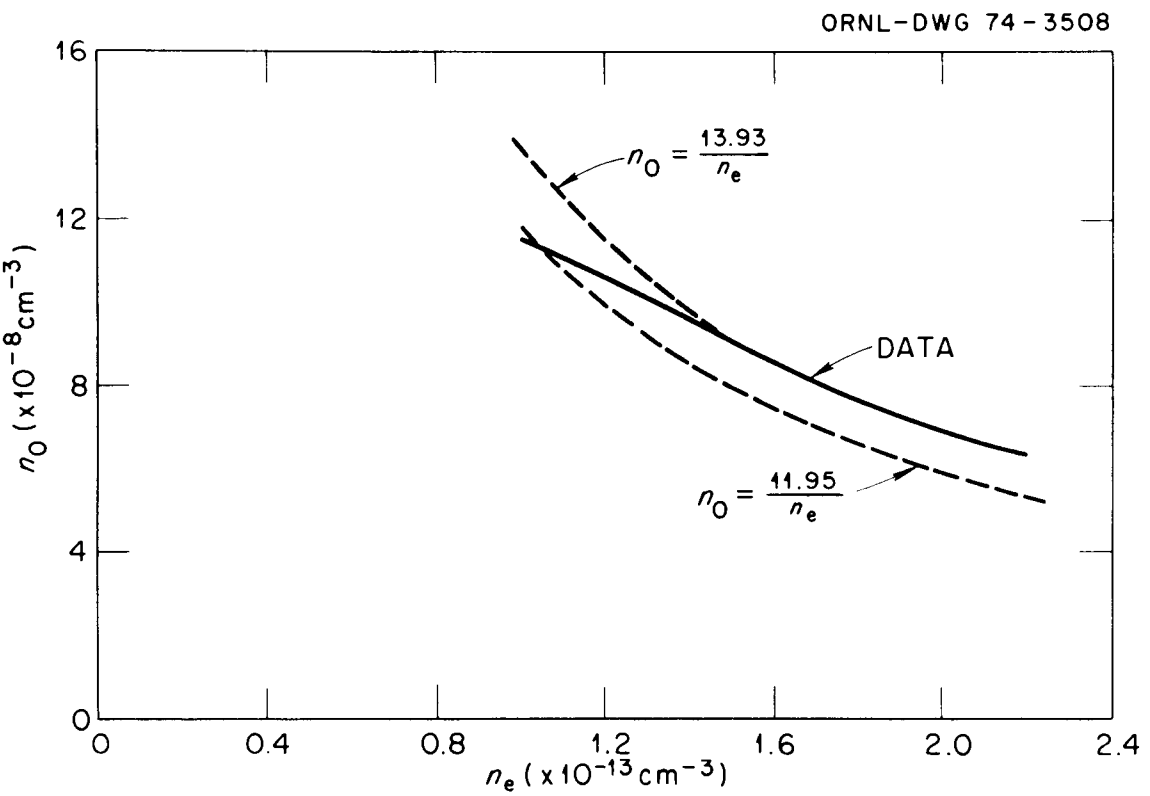

Fig. A3. The dependence of the central neutral density on electron density obtained from a self-consistent solution of our pseudoclassical plasma simulation code and the Boltzmann equation governing the transport of neutral particles is shown by the solid line in the Figure. The simple relationship $n_0 \times n_e$ equal to a constant can fit the data shown within 8%.

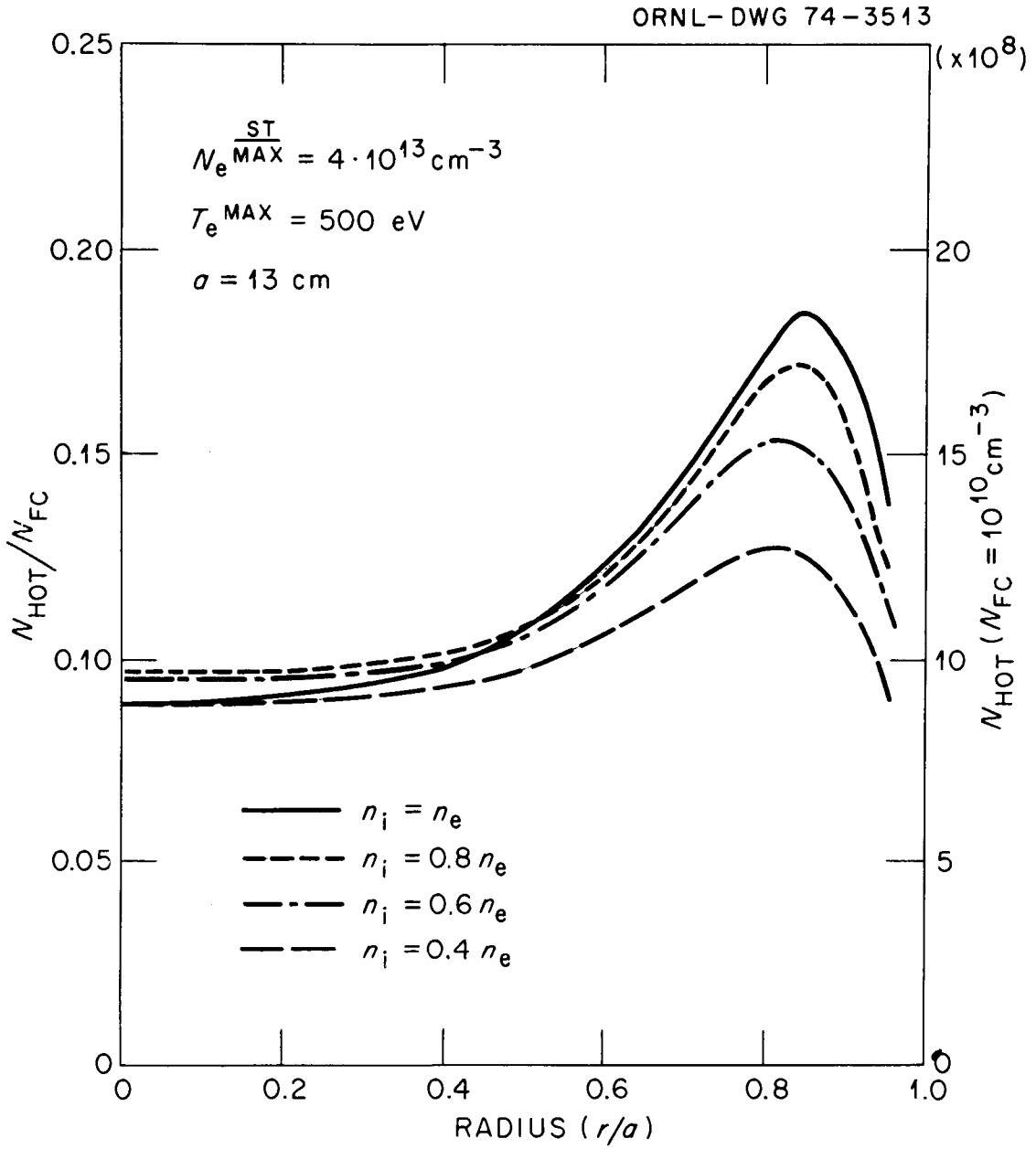

Fig. A4. The central neutral density in the ST plasma as a function of the impurity concentration and radius. Only the surface neutral density is greatly affected by the impurity concentration.

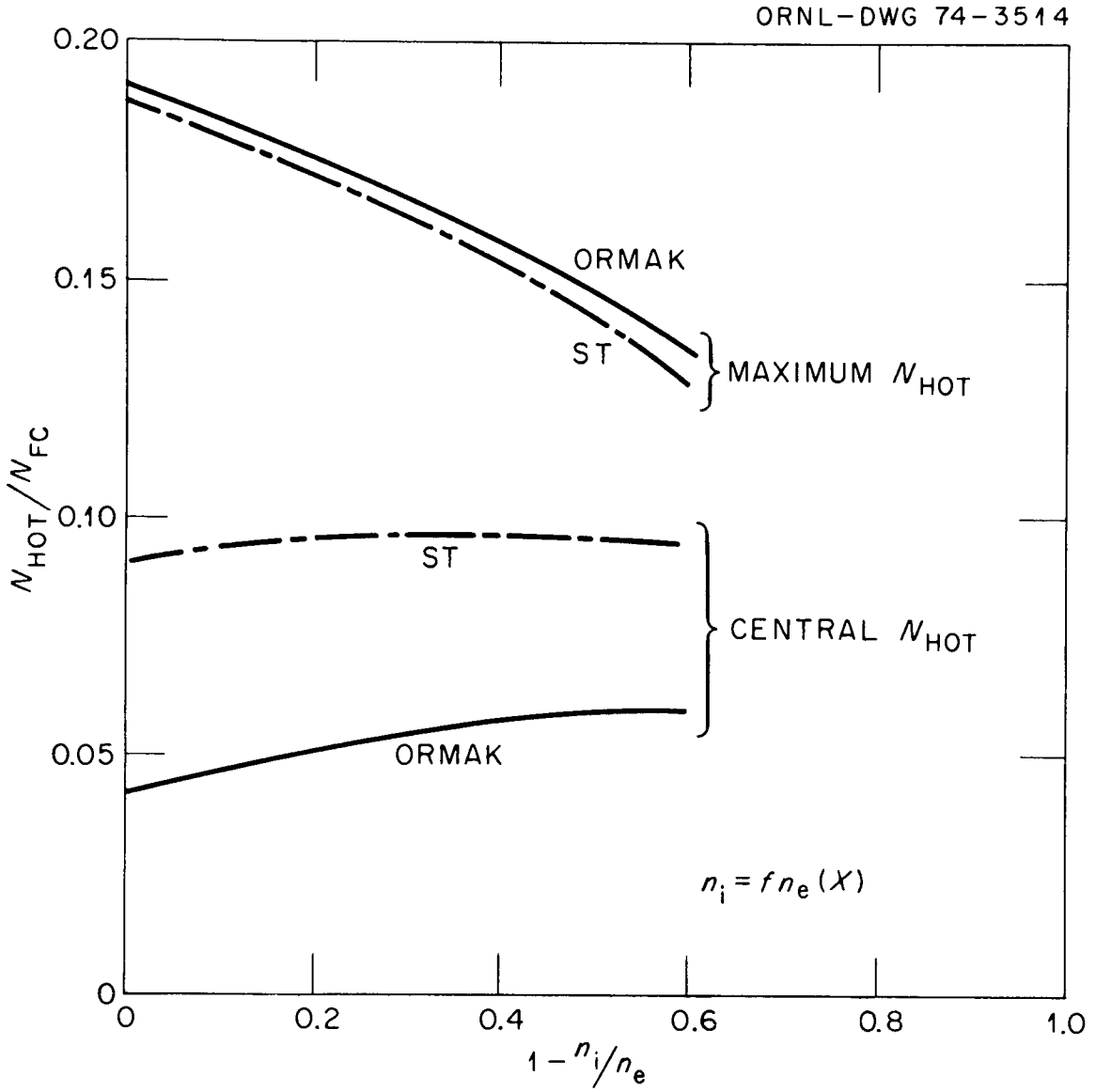

Fig. A5. The maximum and central hot neutral density in the ORMAK and ST plasmas are shown as a function of impurity concentration. Again, the insensitivity of the central neutral density to impurity concentration is evident.

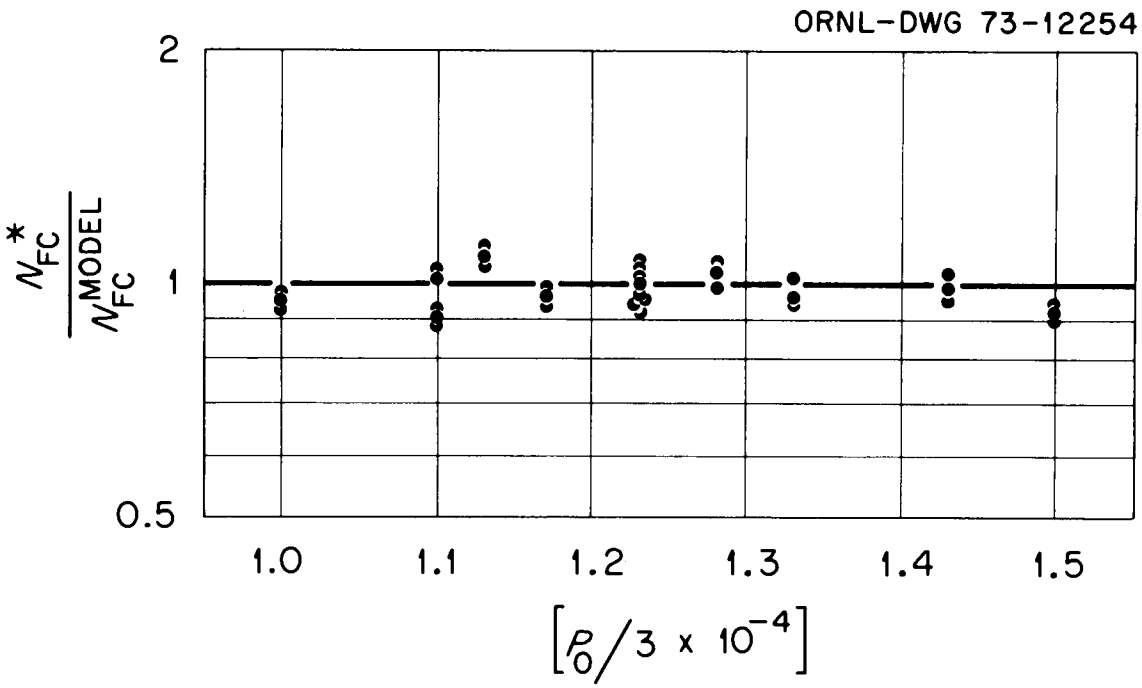

Fig. A6. The Figure shows the ratio of N_{fc}*, which is the surface Frank-Condon density required in order to match the data obtained from our neutral particle spectrometer with the predictions of our neutral transport calculations, to N_{fc}^{model}, the Frank-Condon density directly proportional to the filling pressure in the experiment, as a function of the filling pressure. The data indicate a statistical dependence of the surface Frank-Condon density on the filling pressure with a standard deviation from unity of .1.